CHAPTER 1

LITERATURE REVIEW

1. INTRODUCTION

1.1 Overview of magnetic nanoparticles (MNPs)

Since the mid-1970s, magnetic particles (MPs) from nanometer (nm) to micrometer (μm) size have been widely used in biological and medical fields. The unique feature of magnetic particles is their response to magnetic force. For biomedical applications, magnetic particles exhibiting super paramagnetic behavior at room temperature are preferred because they do not retain any magnetism after removal of the magnetic field (H). Furthermore, the particles (Ps) must have combined properties of high magnetic saturation, biocompatibility and interactive functions at the surfaces. Among magnetic particles, iron oxide (FeO) such as magnetite (Fe_3O_4) or its oxidized from maghemite (Fe_2O_3) are by far the most commonly employed in biomedical applications since their biocompatibility has already been proven (Schwertmann and Cornell, 1991). Highly magnetic materials such as cobalt (Co) and nickel (Ni) are toxic, susceptible to oxidation and hence are of little interest. Magnetite or maghemite nanoparticles (NPs) are usually modified through the formation of a few atomic layers of polymer/surfactant or inorganic metallic (such as gold) or oxide surfaces (such as silica or alumina), which are suitable for further functionalization by the attachment of various biomolecules (Berry and Curtis, 2003). Magnetic particles are either well dispersed in a liquid, i.e., for medical application, or form composites with polymer or inorganic matrices, the so-called magnetic microspheres or beads.

Magnetic particles with suitable surface characteristics have potential applications both *in vitro* and *in vivo*. In almost all applications, the preparation and surface modification of magnetic particles present significant challenges in determining the particles size and shape, the size distribution, the surface chemistry and consequently the magnetic

properties of the particles, all important for biomedicine (Tartaj and Serna, 2003; Tartaj *et al.,* 2003).

In recent years, magnetic nanoparticles have been studied for their potential applications as magnetic carriers for various biomedical uses such as cell and Deoxyribonucleic acid (DNA) separation, drug delivery system (DDS), magnetic resonance contrast enhancement and gene cloning. In particular, magnetic beads with a few micrometers in diameter are already commercialized and used for cell separation, deoxyribonucleic acid isolation and protein isolation. For these applications, their surfaces are coated with a layer to combine with functional bio molecule for each purpose and avoid nonspecific adsorption. However, the commercially available magnetic beads cannot be used as a general purpose carrier. For each bio molecule it is necessary to coat the particles with an appropriate layer. On the other hand, gold nanoparticles (Au NPs) are also widely studied in the field of biotechnology (Seino *et al.,* 2005).

Gold combines firmly with biomolecules possessing mercapto groups and exhibits a characteristic reddish color due to surface plasmon resonance. The color changes when Gold nanoparticles aggregate with the molecules attached on their surface. Thus colorimetric detection of specific biomolecules is possible. The magnetic nanoparticles with ‘shell/core’ structure have attracted great interests as potential candidates for applications in magnetic recording media, catalysis, ferro fluids (FFs), diagnosis, drug delivery (DD) and microwave absorbents. The outer shell can protect metallic magnetic nanoparticles against environmental degradation, and effectively increase the distance of neighboring magnetic nanoparticles, which result in weak magnetic coupling between individual nanoparticles (Zhang *et al.,* 2007).

Magnetic nanoparticles have potential applications in many biological and medical fields such as drug delivery, hyperthermia treatment, magnetic resonance contrast enhancement and cell separation. Even though a biocompatible iron oxide nanoparticle is currently the material of choice, there is significant interest in developing alternative high magnetic moment cobalt (and related alloys) for specific biomedical applications. While the

majority of magnetic nanoparticles prepared at present for biomedical applications are bead-like or spheres, other anisotropic shapes with larger dipole moment per unit volume have been considered for cell manipulation applications. Irrespective of their shape, the challenge here is to prepare uniform, un-agglomerated particles with controlled size, shape and narrow size distribution. However, since metallic cobalt nanoparticles (Co NPs) are highly sensitive to oxidation and are toxic for biological application, it would be highly desirable to coat them with an inert shell for biocompatibility and stability. Further, if the shell could provide additional functionality, such as sensitivity to optical probes and other bio molecules, it would be highly desirable for a number of applications. Gold coating of the magnetic nanocrystals would be a natural choice to accomplish both of these goals (Yuping and Kanna, 2005).

Magnetic nanoparticles have been attractive materials in biology and biomedicine. They have size ranges from a few nm to tens of nm that are comparable to those of a protein; antibody, deoxyribonucleic acid or Ribonucleic acid (RNA), and can interact with or bind to such biomolecules. Magnetic iron-oxide nanoparticles (Fe_3O_4 NPs) are intensively studied as a promising candidate material for these uses because of their high chemical stability and non-toxicity. For these applications, the surface of the particles should be modified by a biocompatible compound such as polyethylene glycol (PEG), polyvinyl alcohol (PVA), dextran, gold or silica (Si). These surface modifications act to shield the magnetic particles from the surrounding environment. To bind the bio molecules onto their surface often requires chemical reactions. On the other hand, gold nanoparticles are also widely studied for biological applications. In general, gold combines firmly with bio molecules possessing thiol (-SH) or mercapto groups, *via* gold-sulphur bonds. Gold nanoparticles exhibit a reddish colour in a colloidal solution due to the surface plasmon absorption. Aggregation of the gold nanoparticles caused by cross-linking, such as during deoxyribonucleic acid hybridization, may change the colour of the colloidal solution to purple, thus making a colorimetric deoxyribonucleic acid detection possible (Kinoshita *et al.,* 2007).

During the past years, the preparation and characterization of nanoscale materials have become an important branch of materials research and attracted considerable attention

from both fundamental and applied research due to their unique, electrical and other properties. To date, a variety of preparative approaches have been investigated and many reviews are now available. Solution-phase syntheses may represent the most promising route to nanoparticles in terms of cost, throughput, and the potential for high-volume production. Unfortunately, unprotected metal colloids are susceptible to irreversible aggregation in solution due to small size. One of the effective strategies is to protect colloids with protective agents, which can spontaneously absorb on the particle surface leading to colloids in which individual particles are separated from each other, preventing them from agglomeration (Yonglan, 2007).

As an emerging active area of contemporary materials science, nanocomposites containing two or more different nanoscale functionalities attract much attention. Interests in this kind of nanomaterials originate not only from the curiosity of scientists who are exploring the mesoscopic world, but also from the ever-increasing demands placed on materials synthesis and performance by nanotechnology. The magnetic core/gold shell nanoparticle, for example, is one of such nanocomposites (Lu *et al.*, 2006).

Nanocomposite materials containing a magnetic phase and another functional phase have been attracting much interest from materials scientists because of many interesting and important scientific and technological aspects (Davis, 2001). In particular, the nanoparticle in which both the phases are included is one of the most challenging targets of materials science because of its vast versatility, for instance, application to the drug delivery and bio detection technologies. However, it is not an easy task to characterize such a complex nanoparticle from the view point of the internal structure and the phase that gives rise to magnetism. Carpenter *et al.* (1999) have reported synthesis of core-shell structured iron (Fe)-gold nanoparticles with an average diameter of 12 nm by the reverse micelle method and proposed many applications. They postulated that their particle is composed of a core of metallic iron and a shell of metallic gold, on the basis of much circumstantial evidence. This group has synthesized super paramagnetic nanocomposite materials composed of magnetic nanograins of iron oxide or nitride dispersed in a silica

matrix by the inert gas condensation method (Yamamoto *et al.,* 1994; Yamamoto *et al.*, 1999), and studied the phase of the iron-containing nanograins giving rise to the magnetism of the grains. The average magnetic moment size and its standard deviation were examined by analyzing the magnetization (M) behavior (Tanaka *et al.,* 2001; Yamamoto *et al.,* 2002), and the phase containing iron was identified by X-ray absorption near edge structure (XANES). (Yamamoto *et al.,* 1995; Nishimaki *et al.,* 2000)

1.2 Immobilization of special molecules on the surface of nanoparticles

There has been extensive investigation of the applications of the immobilization of special molecules on the surface of the nanoparticles (Liu *et al.,* 2003; Liu *et al.,* 2005). For example the immobilization of substrate specific ligands on the surface of nanoparticles can be used for the specific removal or recycling of the substrates (Gong *et al.,* 2007; Ashtari *et al.,* 2005; Gao *et al.,* 2003). Furthermore, because the surface reactions of nanoparticles and those of ligands immobilized on the surface of nanoparticles have dramatic effects on a number of physical, chemical and electronic properties of the nanoparticles, the immobilization of substrate specific ligands on the surface of nanoparticles can also be used for the detection of substrates in mixtures (Zhang *et al.*, 2007). The immobilization of antibodies on the surface of nanoparticles can be used for the detection of specific antigens (Aurich *et al.,* 2007; Liu *et al.,* 2006). The description of core-shell nanoparticles with a super paramagnetic core materials and relatively inert shell materials has introduced several interesting possibilities (Wagner *et al.,* 2002; Zhang *et al.,* 2006). The magnetic core allows for exclusion and/or removal of the nanoparticles by application of a magnetic field strength (Gong *et al.,* 2007; Ashtari *et al.,* 2005; Gao *et al.,* 2003). This can provide a powerful tool for the detection, purification and recycling of substrates, particularly bio-molecules such as deoxyribonucleic acid and proteins (Aurich *et al.,* 2007; Liu *et al.,* 2006).

1.3 Magnetic nanoparticles in biomedical applications

The use of magnetic nanoparticles in biomedical applications requires a non-toxic core material and bio-compatible or bio-inert shell. This can be achieved with a core of super paramagnetic material and a shell of inert material. In addition the shell of inert material may be coated with bio-compatible molecules or molecules with specific bio-responses or bio-activities. In this way, in addition to enhancing this bio-compatibility, the immobilization of bio-compatible ligands on the inert shell can also introduce generic or specific bio-sensitivity. For example the functionalization of magnetic nanoparticles with antibodies in magnetic immunoassays and binding experiments to confirm the bonding capacity and demonstrate the bio-medical applications have been reported (Aurich *et al.,* 2007; Liu *et al.,* 2006). Some of the commonly used core materials include super paramagnetic magnetite of iron oxide (Tie *et al.,* 2007; Wu *et al.,* 2006), ferromagnetic cobalt (Wang and Lee, 2007) and ferromagnetic cobalt platinum (Seto *et al.,* 2006). Probably due to the wide range of available synthetic procedures and magnetic properties, silica has been the coating material of choice (Gong *et al.,* 2007; Ashtari *et al.,* 2005; Gao *et al.,* 2003; Wagner *et al.,* 2002; Zhang *et al.,* 2006; Tie *et al.,* 2007; Wu *et al.,* 2006; Seto *et al.,* 2006), although the use of inert metals, notable gold (Lim *et al.,* 2007; Lu *et al.,* 2006; Carpenter, 2001) and silver (Ag), (Gong *et al.,* 2007) have proved to be quite competitive in recent studies.

1.4 Super paramagnetic Iron Oxide Nanoparticles (SPION)

Super paramagnetic iron oxide nanoparticles are small γ-maghemite or magnetite particles with a size of <10 nm in diameter. The term ‘‘super paramagnetism’’ is used to infer an analogy between the behavior of the small magnetic moment of a single paramagnetic atom and that of the much larger magnetic moment of a nanosized magnetic particles which arises from the coupling of many atomic spins. After eliminating the magnetic field, the particles no longer show magnetic interaction; a feature that is important for their usability (Neuberger *et al.,* 2005). Super paramagnetic iron oxide nanoparticles with appropriate surface chemistry have been widely used

experimentally for numerous *in vivo* applications such as magnetic resonance imaging (MRI) contrast enhancement, tissue repair, immunoassays, detoxification of biological fluids, hyperthermia, drug delivery and in cell separation, etc. All these biomedical and bioengineering applications require that these nanoparticles have high magnetization values and size smaller than 100 nm with overall narrow particle size distribution, so that the particles have uniform physical and chemical properties.

In addition these applications need special surface coating of the magnetic particles, which has to be not only non-toxic and biocompatible, but also allow a targetable delivery with particle localization in a specific area. Most work in this field has been done in improving the biocompatibility of the materials, but only a few scientific investigations and developments have been carried out in improving the quality of magnetic nanoparticles, their size distribution, their shape and surface in addition to characterizing them to get a protocol for the quality of these particles (Gupta and Gupta, 2005).

Iron oxide (usually magnetite and maghemite) nanoparticles are mostly used as magnetic particles in ferro fluids due to their high saturation magnetization (*M*s) and high magnetic susceptibility. Magnetite particles are preferred because of their greater saturation magnetization. The nanoparticles need to be stabilized in the carrier liquid because they tend to agglomerate due to van der waals forces (Maity and Agrawal, 2007).

1.5 Synthesis of magnetic iron oxide nanoparticles

The preparation and synthesis of magnetite nanoparticles can be divided into physical methods such as gas phase deposition and electron beam lithography, wet chemical methods and biological methods (Tartaj and Serna, 2003; Tartaj *et al.,* 2003). Among them, wet chemical methods are widely used due to their straightforward nature and ease of control over size; composition and even the shape of the nanoparticles. Co-precipitation is by far the most commonly used method for the preparation of magnetite nanoparticles for biotechnology. There are two main methods for the synthesis of both

magnetite and γ-maghemite nanoparticles in solution. In the first, ferrous hydroxide $Fe(OH)_2$ suspensions are partially oxidized with different oxidizing agents, such as nitrate ions (Sugimoto and Matijevi, 1980), aqueous hydrogen peroxide (H_2O_2) solution (Winnik *et al.*,1995), ‘‘spontaneously’’ in an open atmosphere or else in an inert atmosphere (Yaacob *et al.,* 1994). The other consists in the co-precipitation of Fe^{2+} to Fe^{3+} aqueous salt solutions by the addition of a base (Khalafalla and Reimers, 1980). The control of size, shape and compositions of nanoparticles depends on the type of salts used, Fe^{2+} and Fe^{3+} ratio, pH and ionic strength of the precipitation medium (Qiu, 2000; Vayssieres *et al.,* 1998; Liu *et al.,* 2004). The disadvantage of these bulk solution syntheses is that the pH of the reaction mixture needs to be adjusted during synthesis. The production of large quantities of magnetic nanoparticles with a narrow size distribution remains a significant challenge for these methods.

Some new methods with better control of size distribution of magnetic nanoparticles have recently been developed. These include the micro emulsion method and high-temperature decomposition of organic precursors. A micro emulsion is a transparent, isotropic, and thermodynamically stable liquid medium. In water-in-oil (W/O) micro emulsion, the fine micro droplets of the aqueous phase are trapped within assemblies of surfactant molecules dispersed in a continuous hydrocarbon phase. The surfactant-stabilized micro cavities provide a confinement effect that limit particle nucleation, growth, and agglomeration. Micro emulsions have been successfully used as nanoreactors for the synthesis of magnetic nanoparticles. Lopez-Quintela and Rivas (1993) and Gupta and Wells (2004) prepared magnetic nanoparticles of 4 nm and 15 nm with narrow size ranges and uniform chemical and physical properties using aqueous core of aerosol-[OT](AOT)/n-hexane reverse micelles (W/O micro emulsions), respectively. The nanoparticles exhibit super paramagnetic behavior with high magnetization values reaching 40-50 emu/g. The principal advantage of the micro emulsion system is that the size of nanoparticles can be controlled by varying their composition and by modulating the size of the aqueous micellar core. However, there are several disadvantages of using micro emulsion for the synthesis of magnetic nanoparticles. First, extensively agglomerated nanoparticles are often generated. Second, the nanoparticles are poorly

crystalline for the procedure is usually performed at a relatively low temperature. Third, the yield of the nanoparticles is often very low. To overcome these, Lee *et al.* (2005) developed the novel micro emulsion methods performed at high temperature (90°C) for the synthesis of large amounts of magnetic nanoparticles ranging from 2 to 10 nm with uniform size distribution by adjusting the concentration of iron salt or the surfactant.

The decomposition of iron precursors in the presence of hot organic solvents has yielded nanoparticles with narrow size distribution, good crystallinity and dispersibility. For example, Rockenberger *et al.* (1999) synthesized γ-maghemite nanoparticles ranging from 4-10 nm in diameter from the direct decomposition of Fe $(Cup)_3$ (where Cup: N-nitrosophenylhydroxylamine) in octylamine at 250-300°C. Sun and Zeng (2002) prepared monodispersed magnetite nanoparticles with size from 3 to 20 nm by the high-temperature reaction of iron (III) acetyl acetone, Fe $(C_5H_7O_2)_3$. Although they produced highly crystalline and uniform magnetic nanoparticles, this method cannot be applied to large scale and economic production, because they usually use expensive and toxic reagents, complicated synthetic steps, and high reaction temperature.

There are various chemical methods aimed at synthesizing magnetic nanoparticles for a wide range of applications. LaConte *et al.* (2005) focused on synthesis methods that have been adapted from the analysis of magnetic nanoparticles used for medical imaging applications. The most commonly used methods to form iron oxide nanoparticles use a precipitation-based synthesis approach, which is done by co-precipitation on reverse micelle synthesis. Although the co-precipitation method can vary the average size of nanoparticles by adjusting pH and the temperature of aqueous media, it has only limited control over the size distribution of the particles. On the other hand, reverse micelle synthesis, can produce very uniform particles (<10% variability). Since the magnetic nanoparticles produced using reverse micelle method are soluble only in organic solvents, this technique has not been commonly used for biomedical applications. To overcome this difficulty, in a recent study by Nitin *et al.* (2004), a coating procedure was developed to render these uniformly sized nanoparticles water-soluble. A new development in magnetic nanoparticle synthesis is the ability to produce a large amount (~ 40g) of

monodisperse magnetic nanoparticles using metal salts as reactants. This method allows precise control of nanoparticle size (with size variation < 5%) simply by varying the experimental conditions such as temperature and concentration, which is a distinct improvement over other methods.

It has long been of scientific and technological challenge to synthesize the magnetic nanoparticles of customized size and shape. Iron oxide (either magnetite or maghemite) can be synthesized through the co-precipitation of Fe^{2+} and Fe^{3+} aqueous salt solutions by addition of a base (Reimers and Khalafalla, 1972). The control of the size, shape and composition of nanoparticles depends on the type of salts used (e.g. chlorides, sulphites, nitrates, perchlorates, etc), Fe^{2+} and Fe^{3+} ratio, pH and ionic strength of the media (Sjogren *et al.,* 1994). Conventionally, magnetite is prepared by adding a base to an aqueous mixture of Fe^{2+} and Fe^{3+} chloride at a 1:2 molar ratio. The precipitated magnetite is black in color. The chemical reaction of magnetite precipitation is given as follows:

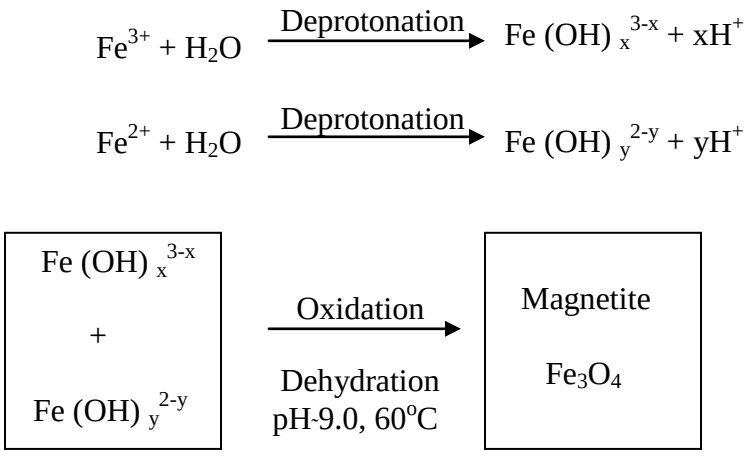

Figure. 1. Scheme showing the reaction mechanism of magnetite particle formation from an aqueous mixture of ferrous and ferric chloride by addition of a base (NH_4OH). The precipitated magnetite is black in colour.

The overall reaction may be written as follows:

$Fe^{2+} + 2Fe^{3+} + 8OH^- \rightarrow Fe_3O_4$ (black colloidal particles) + $4H_2O$……... (1)

According to the thermodynamics of this reaction, a complete precipitation of magnetite should be expected between pH 9 and 14, while maintaining a molar ratio of Fe^{3+}:Fe^{2+} of 2:1 under non-oxidizing oxygen (O_2) free environment. Otherwise, magnetite might also be oxidized as

$$4Fe_3O_4 + O_2 + 18H_2O \rightarrow 12Fe(OH)_3 \quad \ldots\ldots (2)$$

This would critically affect the physical and chemical properties of the nanosized magnetic particles. In order to prevent them from possible oxidation in air as well as from agglomeration, magnetite nanoparticles produced by reaction (1) are usually coated with organic or inorganic molecules during the precipitation process. To control the reaction kinetics, and therefore the oxidation speed of iron species, the synthesis of particles must be done in an oxygen-free environment by passing nitrogen (N_2) gas. Bubbling nitrogen gas through the solution not only protects critical oxygen of the magnetite but also reduces the particle size when compared with methods without removing the oxygen (Gupta and Curtis, 2004; Kim *et al.*, 2001).

1.6 Surface modifications of magnetic nanoparticles for biomedical applications and their effect on stability and magnetization

In the preparation and storage of nanoparticles in colloidal form, the stability of the colloid is of utmost importance. Ferro fluids are colloidal suspensions of magnetic nanoparticles (magnetite or maghemite), forming magnetizable fluids (Fs) that remain liquid in the most intense magnetic field. As a result of their composition, the magnetic fluids (MFs) possess a unique combination of fluidity and the capability to interact with a magnetic field (Bailey, 1983; Charles and Popplewell, 1980; Khalafalla and Reimers, 1980). In the absence of any surface coating, magnetite particles have hydrophobic surfaces with a large surface area to volume ratio. Due to hydrophobic interactions between the particles, these particles agglomerate and form large clusters resulting in increased particle size. These clusters, then, exhibit strong magnetic dipole-dipole attractions between them and show ferromagnetic behaviour (Hamley, 2003). When two large particles clusters approach one another, each of them comes into the magnetic field

of the neighbour. Besides the arousal of attractive forces between the particles, each particle is in the magnetic field of the other and gets further magnetized (Tepper *et al.*, 2003).

The adherence of remnant magnetic particles causes a mutual magnetization, resulting in increased aggregation properties. Since particles are attracted magnetically, in addition to the usual flocculation due to van der waals forces, surface modification is often indispensable. For effective stabilization of iron oxide nanoparticles, often coating is desirable. Some stabilizer such as a surfactant or a polymer is usually added at the time of preparation to prevent aggregation of the nanoscale particulate. Most of these polymers adhere to surfaces in a substrate specific manner (Mendenhall *et al.*, 1996). A scheme showing different strategies for fabrication and surface modification of magnetite nanoparticles is shown in the figure below.

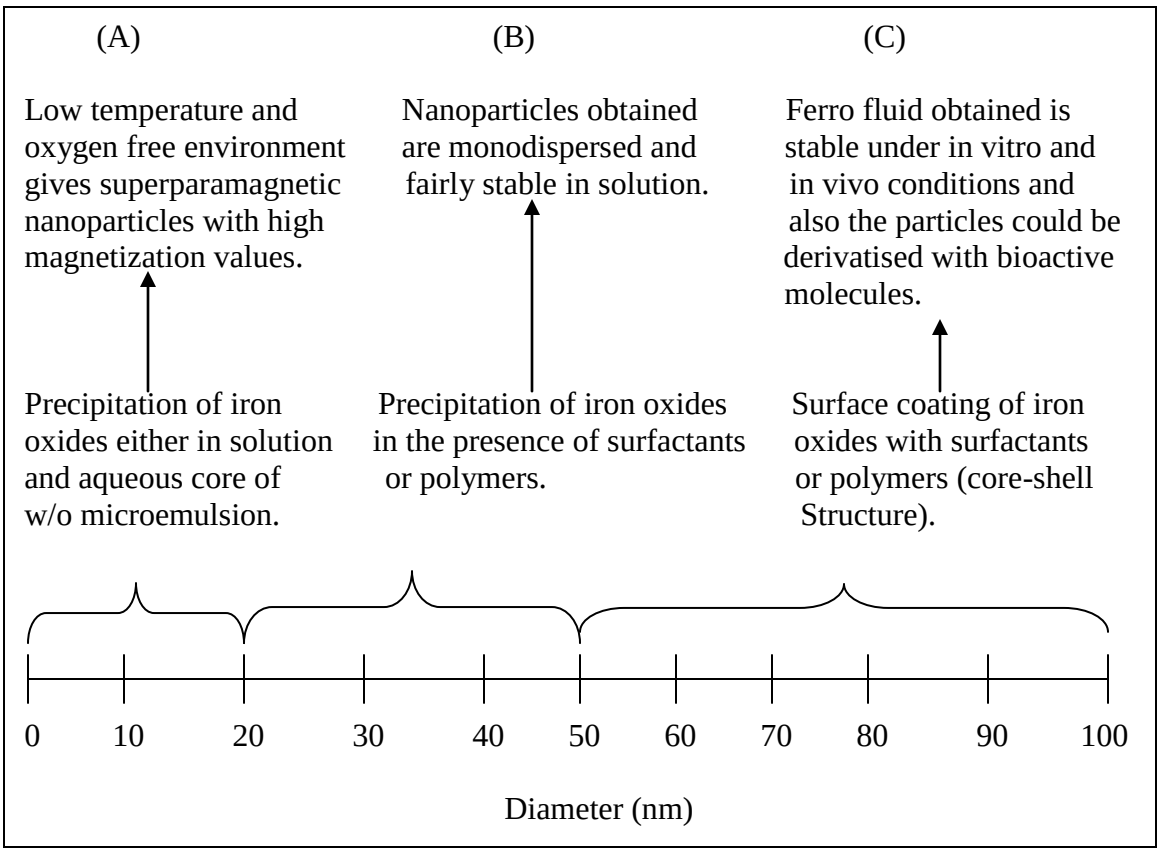

Figure. 2. Scheme showing different strategies for fabrication and surface modification of magnetite nanoparticles. Smaller and more uniform nanoparticles can be prepared inside the aqueous droplets of reverse micelles.

1.6.1 Surface modification with non-polymeric organic stabilizers

In order to stabilize the colloidal dispersion, Gedanken studied the adsorption of alkanesulphonic and alkanephosphonic acids on the surfaces of amorphous magnetite nanoparticles and proposed two possible bonding schemes for the phosphonate ions on Fe^{3+}, i.e., one or two oxygen atoms of the phosphonate groups binding onto the surface (Yee *et al.,* 1999). Sahoo *et al.* (2001) have reported the surface derivatization of magnetite by oleic acid, lauric acid.etc, to stabilize the nanoparticles in organic solvents. They found that alkyl phosphonates and phosphates could be used for obtaining thermodynamically stable dispersions of magnetic nanoparticles. The authors suggested on the basis of the results obtained from the temperature and enthalpy desorption studies

that these ligands form a quasi-bilayer structure with the primary layer strongly bonded to the surface of the nanoparticles (Tadmor *et al.,* 1997).

1.6.2 Surface modification with polymeric stabilizers

Various biological molecules such as antibodies, proteins, targeting ligands, etc., may also be bound to polymer surfaces on the nanoparticles by chemically coupling *via* amide (R_1 (CO) NR_2R_3) or ester (R-COOR′) bonds to make the particles target specific. Polymeric coatings on magnetic nanoparticles offer a high potential in several areas of applications. Precipitation of inorganic particles in a cross-linked polymer matrix or network of gel often prevents coagulation of particles, giving rise to monodisperse particles (Berry *et al.,* 2003; Gupta and Hung, 1989). The pioneering work of Ugelstad *et al.* (1993) based on the preparation of hydrophobic monosized polystyrene magnetic nanoparticles, has stimulated the research in this domain. Lee *et al.* (1996) have modified nanoparticles's surface with poly vinyl alcohol by precipitation of iron salts in poly vinyl alcohol aqueous solution to form stable dispersion. They found that the crystallinity of the Ps decreased with increasing poly vinyl alcohol concentration, while the morphology and particle size remained unchanged (Ng *et al.,* 2002).

1.6.3 Surface modification with inorganic materials

Metallic core-shell types of iron oxide nanoparticles have been investigated by several researchers. These nanoparticles have inner iron oxide core with an outer metallic shell of inorganic materials. The iron oxide nanoparticles have been coated with silica, gold or gadolinium, etc. This coating provides not only the stability to the nanoparticles in solution but also helps in binding the various biological ligands at the nanoparticles surface for various biomedical applications. Chen *et al.* (2003) synthesized two kinds of gold-coated iron based particles: a circular and spherical, and studied the effect of heat treatment in acid on the coercivity and saturation magnetization of the particles. The gold-coated circular particles had initial coercivities very close to those of the uncoated sample, and the changes after heating in acid were small. The relative saturation magnetization after treatment was higher than for the uncoated particles, indicating at

least partial passivation of the iron. The uncoated spherical iron-based particles were super paramagnetic at room temperature, but the gold-coated spherical particles had a very small coercivity due to slight oxidation during the coating process. While the relative magnetization decreased, the particle moment was still greater than would be expected for pure iron oxide. The gold also provides a good surface for subsequent functionalization with chemical or biological agents (Lin *et al.,* 2001). Magnetic nanoparticles designed for drug delivery must also be completely biocompatible. Iron oxide nanoparticles are known to be non-toxic, and are eventually broken down to form blood haemoglobin. Carpenter *et al.* (2001) prepared metallic iron particles covered by a thin layer of gold via a micro emulsion. The gold shell protects the iron core against oxidation and also provides functionality, making these composites applicable in biomedicine. Several authors have reported the magnetite nanoparticles coated with silica (Ulman, 1996; Mulvaney *et al.,* 2000; Tartaj *et al.,* 2002; Tartaj *et al.,* 2001; Santra *et al.,* 2001). An advantage of having a surface enriched in silica is the presence of silanol groups that can easily react with alcohols (OH) and silane (SiH_4) coupling agents (Ulman, 1996) to produce dispersions that are not only stable in non-aqueous solvents but also provide the ideal anchorage for covalent bonding of specific ligands (Mulvaney *et al.,* 2000).

1.6.4 Surface modifications with targeting ligands

Various biological molecules such as antibodies, proteins, targeting ligands, etc., may also be bound to the polymer surfaces onto the nanoparticles by chemically coupling via amide or ester bonds to make the particles target specific. The possibilities of targeting protein coatings are numerous. Some interesting ligands with regard to targeting cell surface receptors are provided in the table below (Gupta and Gupta, 2005). Linker molecules such as 1-ethyl-3-(3-dimethylaminopropyl) carbodi-imide hydrochloride (EDCI), N-succinimidyl 3-(2-pyridyldithio) proprionate (SPDP), N-hydroxysuccinimide or N,N'methylene bis acrylamide (MBA) are usually used to attach the initial hydrophilic coated molecules to a protein coating aimed at cell surface attachment (Roberts *et al.,* 2002).

Protein/ligand	Functionality activity
Insulin	A hormone that regulates blood glucose levels, is a small protein
Nervegrowth factor (NGF)	Promotes neurite outgrowth and neural cell survival
Ceruloplasm	Principal carrier of copper in plasma, which plays an important role in iron homeostasis and is also an effective anti-oxidant for variety of free radicals
Pullulan	High water soluble, no toxicity, usefulness as a plasma expander, non-immunogenic, non-antigenic properties. Also, evidences for receptor-mediated hepatic uptake of pullulan in rats
Elastin	A cross-linked protein in the extra cellular matrix that provides elasticity for many tissues
Albumin	The major serum protein, binds a wide variety of lipophilic compounds including steroids etc
Tat-peptide	Membrane-permeating peptide, enhances intracellular delivery
RCD peptide	Increases cell spreading, differentiation, and enhances deoxyribo nucleic acid synthesis
Folic acid	Preferentially target cancer cells, poorly immunogenic, folate receptor facilitates internalization of particles

Table 1. Table of selected proteins/targeting ligands that could be used for derivatizing magnetic nanoparticles for various biomedical applications.

1.6.5 Magnetic properties of iron oxide nanoparticles

Sato *et al.* (1987) suggested that the loss of magnetization as the particle size decrease depends largely on the crystalline magnetic anisotropy energy constant, *K*. Smaller anisotropy energy constants display lower relative magnetization values (Sato *et al.*, 1987). Experimental analyses including microscopy, X-ray diffraction (XRD) and magnetometry studies suggest that the reduced magnetization is due to surface characteristics of nanoparticles. Specifically, the loss of magnetization may be due to the existence of a magnetically dead layer, $\sim$1 nm thick, caused by an asymmetric environment effect of the surface atoms (Sato *et al.,* 1987). Particles made from iron oxide usually behave differently in magnetic fluids depending on their size. It was reported previously by several researchers (Lefebure *et al.,* 1998) and (Bean and Livingstone, 1959) that abrupt changes in magnetic properties take place when the sizes of the particles are reduced from micrometer to nanometer size range. For example, particles have super paramagnetic behaviour when the size is sufficiently small (i.e. 6–15 nm) and they behave as ferromagnetic when the grain size is in micrometer range. It was shown by Chatterjee *et al.* (2003) that the magnetic behaviour is dependent on the blocking temperature (T_B) of the particles (Blocking temperature is the transition temperature between the ferromagnetic and super paramagnetic state and is directly proportional to the size of the particles), which in turn is dependent on the size of the particles. Particles with lower blocking temperature exhibited super paramagnetic properties, whereas the higher blocking temperature of the particles showed the ferromagnetic behaviour of the particles.

Despite the increase in super paramagnetic behaviour of the particles with decrease in particle size, several authors have reported a decline in the absolute saturation magnetization values when the size of the particle is reduced to less than 10 nm (Li *et al.*, 2002) and (Han *et al.,* 1994). Surface modification of the iron oxide usually leads to the formation of a non-magnetic shell due to the formation of particle outer layer and the thickness of such a layer could be in the order of 1–20 nm (Tourinho *et al.,* 1989). The coating of particles with non-magnetic materials may result in decrease of saturation magnetization values. Gomez-Lopera *et al.* (2001) found that surface coverage of poly

(lactide-co-glycolide) polymer on the iron oxide nanoparticles decreased the saturation magnetization of particles to about one-half of that of the pure magnetite and the initial magnetization–magnetic field dependence is steeped in this case. Voit *et al.* (2001) also observed similar results. They studied the magnetic behaviour of super paramagnetic iron oxide nanoparticles in ferro fluids coated with different polymers such as sodium oleate, poly vinyl alcohol or starch. They found that surface coverage of the iron oxide with either of these polymers resulted in decreased saturation magnetization values of the particles. They also observed that the values of particle sizes calculated from the magnetization data are found to be lower than the values calculated by x-ray diffraction and Transmission Electron Microscopy (TEM) measurements, which may be attributed to a magnetically ineffective layer on the particle surface (Bradbury *et al.*, 1984).

Characteristics of the iron oxide	**Preparation Method Synthesis of iron oxide nano-particles prepared through**				
	Aerosol/ vapour (pyrolysis) method	**Gas deposition method**	**Bulk solution method**	**Sol-gel method**	**Micro emulsion method**
Size and size distribution	About 5-60 nm with broad distribution	About 5-50 nm with narrow size distribution	About 10-50 nm with broad size distribution	About 20-200 nm with broad size distribution	About 4-15 nm with very narrow size distribution
Morphology	Spherical	Spherical	Spherical (large aggregates)	Spherical with high porosity	Cubic or spherical (no aggregation)
Magnetization values	10-50 emu/g with desired magnetic property	>20 emu/g	20-50 emu/g with super paramagnetic behavior	10-40 emu/g with paramagnetic behavior	>30 emu/g with super paramagnetic behavior
Advantages	High production rate	Useful for protective coatings and thin film deposition	Large quantities can be synthesized	Particles of desired shape and length can be synthesized, useful making hybrid nanoparticles	Uniform properties and also size of the nanoparticles can be modulated

Disadvantages	large aggregates formed	Require very high temperatures	Uncontrolled oxidation of magnetite maghemite, diamagnetic contribution	Product usually contains sol-gel matrix components at their surfaces	Surfactants are difficult to remove, only a small quantities of iron oxide can be synthesized

Table 2. Comparison of different characteristic features of the iron oxide nanoparticles fabricated through different methods.

1.7 BIOMEDICAL APPLICATIONS OF MAGNETIC NANOPARTICLES

1.7.1 Cellular labelling/cell separation

Cell labelling with ferro/paramagnetic substances is an increasingly common method for *in vivo* cell separation (Olsvik *et al.,* 1994) as the labelled cells can be detected by magnetic resonance imaging (Yeh *et al.,* 1993). Most current labelling techniques utilize either of two approaches: (a) attaching magnetic particles to the cell surface (Handgretinger *et al.,* 1998), (figure 3a) or (b) internalizing biocompatible magnetic particles by fluid phase endocytosis (Schoepf *et al.,* 1998), or phagocytosis (Weissleder *et al.,* 1997). A variety of potential ligands have been conjugated to nanoparticle surfaces to facilitate receptor-mediated endocytosis of the particles, including monoclonal antibodies (Mabs) (Weissleder *et al.,* 1997), (figure 3b). The derivatized nanoparticles act as cellular markers that are targeted at the surface receptors expressed on human fibroblasts surface without being internalized

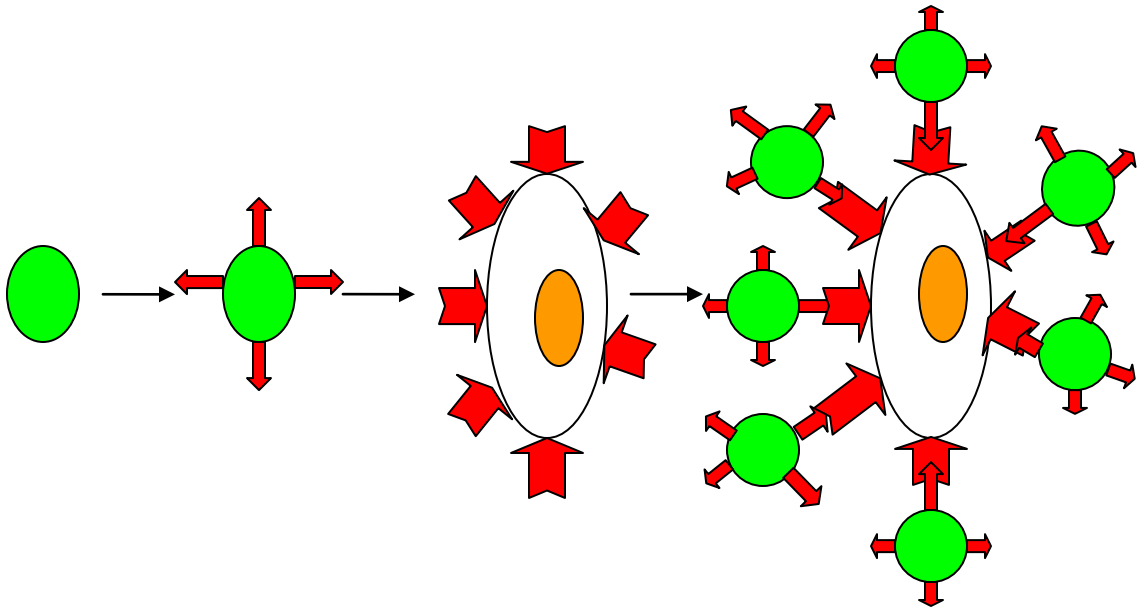

Uncoated magnetic nanoparticle	L_f or C_p derivatized magnetic	Fibroblasts having receptors expressed on their surface for ligand targeting.	Nanoparticles binds to the receptors of the cell surface without being itself internalised

Figure. 3. Scheme of derivatization of super paramagnetic iron oxide nanoparticles either with targeting ligands such as lactoferrin (Lf) or ceruloplasmin (Cp) and their targeting to human fibroblasts. (Gupta and Curtis, 2003; Gupta *et al.*, 2003; Gupta and Curtis, 2004).

1.7.2 Tissue repair

Tissue repair using iron oxide nanoparticles is accomplished either through welding opposing two tissue surfaces then heating the tissues sufficiently to join them, or through soldering, where protein or synthetic polymer-coated nanoparticles are placed between two tissue surfaces to enhance joining of the tissues (Lobel *et al.*, 2000). Nanoparticles that strongly absorb light corresponding to the output of a laser are also useful for tissue-repairing procedures. Specifically, gold-or silica-coated iron oxide nanoparticles have been designed to strongly absorb light (Xu *et al.*, 2004; Sokolov *et al.*, 2003).

The super paramagnetic nanoparticles could be coupled to specific cells and used to target these cells at the desired site in the body. In addition, various proteins, growth

factors, etc., could be bound to these nanoparticles and delivered at the damaged tissue, where it would play a role in tissue development. While there is no doubt that the use of stem cells in the form of cell-based therapies offers tremendous potential for disease including diabetes, cancer, heart disease, Alzheimer's and Parkinson's disease, central to this process would be the ability to target and activate these stem cells at required sites of injury and repair using magnetic particle technology (Bulte *et al.*, 2001).

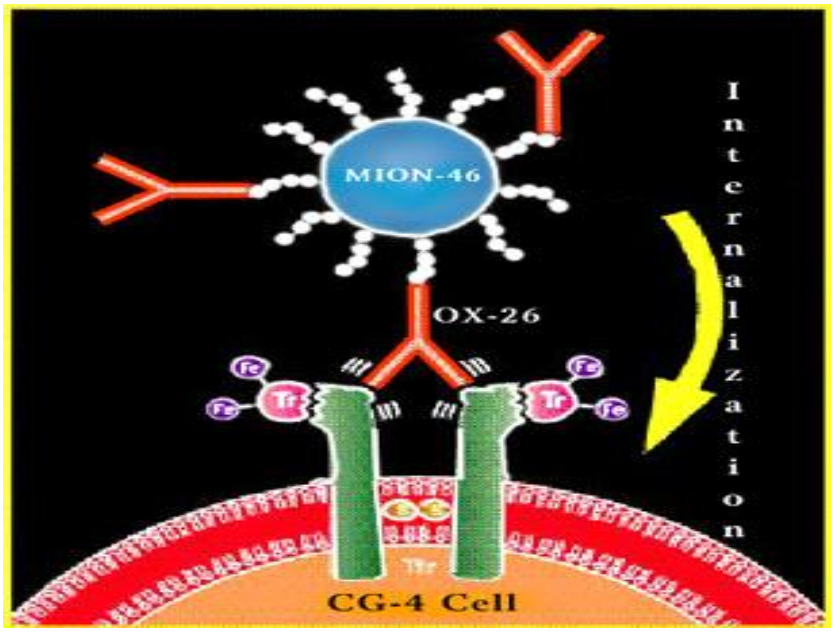

Figure. 4. Internalisation of magnetic particles via monoclonal antibodies and transferrin receptors. Original magnetic tagging system developed by the Laboratory of Diagnostic Radiology Research (LDRR) team and their colleague's shuttles nanoparticles of iron oxide (MION-46L) into cells via monoclonal antibody (OX-26) to the cell's transferrin receptors (Hooper, 2000).

1.7.3 Drug delivery

Another possible and most promising application of these colloidal magnetic nanoparticles is in drug delivery as carriers of drug for site-specific delivery of drugs. Ideally, they could bear either on or in their bulk a pharmaceutical drug that could be driven to the target organ and released there. For these applications, the size, charge and

surface chemistry of the magnetic particles are particularly important and strongly affect both the blood circulation time as well as bioavailability of the particles within the body (Chouly *et al.*, 1996).

In addition, magnetic properties and internalization of particles depend strongly on the size of the magnetic particles (Chatterjee *et al.*, 2003). A number of authors have described the preparation of particles or liposome's containing a certain amount of magnetite or other ferrites. Some of them have focused on the field of drug transport and release: thus, the use of albumin with entrapped magnetite has been studied for the release of anti-cancer drugs like mitomicin and adriamicin (Kubo *et al.*, 2000; Kubo *et al.*, 2001). The attachment of drugs to magnetic nanoparticles can be used to reduce drug doses and potential side effects to healthy tissues and the costs associated with drug treatment.

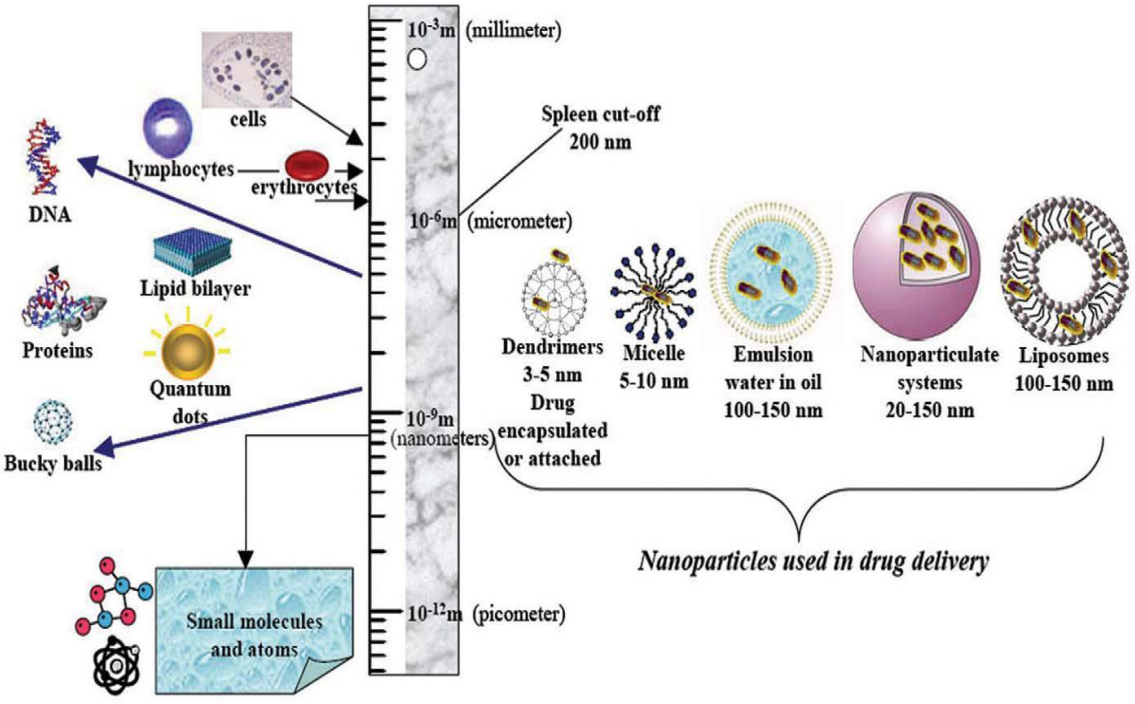

Figure. 5. Nanoparticle systems for drug delivery applications (Tomalia, 2005; Boyd, 2005).

1.7.4 Magnetic resonance imaging (MRI)

Super paramagnetic iron oxide nanoparticles play an important role as magnetic resonance imaging contrast agents, to better differentiate healthy and pathological tissues. Recent developments in magnetic resonance imaging have enabled *in vivo* imaging at near microscopic resolution (Johnson, 1993). Clinical diagnostics with magnetic resonance imaging has become a popular non-invasive method for diagnosing mainly soft tissue or recent cartilage pathologies, because of the different relaxation times of hydrogen atoms (Moghimi *et al.,* 2001; Vladimir *et al.,* 1999). Super paramagnetic iron oxide nanoparticles were developed as contrasts agents for magnetic resonance imaging and increase the diagnostic sensitivity and specificity due to modifications of the relaxation time of the protons (Moghimi *et al.,* 2001; Arbab *et al.,* 2003; Berry and Curtis, 2003). The first dextran coated super paramagnetic imaging was already 10 years ago officially registered as contrast agents for magnetic resonance imaging of the liver in Europe (Reimer and Weissleder, 1996). The efficacy of the super paramagnetic iron oxide nanoparticles as contrast agents in various tissues depends on their physicochemical properties, such as size, charge and coating (Tillotson *et al.,* 2001), and can be increased through surface modifications by biologically active substances (antibodies, receptor ligands, polysaccharides, proteins., etc). (Moghimi *et al.,* 2001, Arbab *et al.,* 2003, Torchilin and Trubetskoy, 1995).

The hydrodynamic diameter of the super paramagnetic iron oxide nanoparticles used with magnetic resonance imaging varies between 20 and 3500 nm, although intravenously applied particles are relatively small and range between 20 and 150 nm with, or 5-15 nm without coating (Goya *et al.,* 2003; Sahoo *et al.,* 2001). Super paramagnetic iron oxide nanoparticles are predestined for use as combined carrier systems for drug delivery while at the same time serving as contrast agent (Arbab *et al.,* 2003). In this way, the kinetics of the pharmaceutical agent could be followed by means of magnetic resonance imaging. In addition, distribution of particles can be influenced through the application of an external magnet (Chatterjee *et al.,* 2003). Most iron oxides have a relatively short half-life and their primary application is for imaging of liver, spleen and Gastrointestinal (GI) tract. Surface-modified iron oxide nanoparticles having long blood circulation times, however,

may prove very useful for imaging of the vascular compartment (magnetic resonance angiography), imaging of lymph nodes, perfusion imaging, receptor imaging and target specific imaging (Weissleder *et al.*, 1995).

1.7.5 Hyperthemia

Through the oscillation of the magnetic moment inside the particles the magnetic field energy is liberated in the form of heat and conducted to the tissue environment (Moghimi *et al.*, 2001). The use of hyperthemia (heat) in the treatment of malignant tumors is as old as medicine itself. For example, Hippocrates, the father of medicine, proposed that surface tumors should be cauterized by application of hot iron. In modern times, more advanced methods (hot water bath, pyrogens such as mixed bacterial toxins, perfusion heating, high-frequency radiation, magnetic fluid hyperthemia) were employed to heat, and hopefully destroy, tumors (Nielsen *et al.*, 2001). Magnetic induction hyperthemia (MIH) is one of the therapies for cancer treatment, means the exposition of cancer tissues to an alternating magnetic field strength. Magnetic field strength is not absorbed by the living tissues and can be applied to deep region in the living body. When magnetic particles are subjected to a variable magnetic field strength, some heat is generated due to magnetic hysteresis loss. The amount of heat generated depends on the nature of magnetic material and of magnetic field strength parameters. Magnetic particles embedded around a tumor site and placed within an oscillating magnetic field strength will heat up to a temperature dependant on the magnetic properties of the material, the strength of the magnetic field, the frequency of oscillation and the cooling capacity of the blood flow in the tumor site. Cancer cells are destroyed at temperature higher than 43˚C; where as the normal cells can survive at higher temperatures. Heat could be generated applying an appropriate magnetic field strength. The size of the magnetite crystals is sub micrometric, so the powders or bulk of these biomaterials have comparable properties. These materials are not only biocompatible but also bioactive and could be useful for bone tumors (Gordon *et al.*, 1979). Much work using magnetic particles for hyperthemia has already been done in order to manifest a therapeutic effect on several types of tumors by performing experiments with animals (Luderer *et al.*, 1983) or using cancerous cell cultures (Chan *et al.*, 1993).

1.7.6 Magnetofection

Magnetofection (MF) is a method in which magnetic nanoparticles associated with vector deoxyribonucleic acid are transfected into cells by the influence of an external magnetic field. For this purpose, magnetic particles might be coated with the polycation polyethylenimine (PEI). These complexes readily associate with negatively charged deoxyribonucleic acid since the magnetic nanoparticles are positively charged due to the polyethylenimine. Whether viral or nonviral vectors, magnetofection has been shown to enhance the efficiency of the vectors up to several thousand times (Scherer *et al*., 2002). For magnetically enhanced nucleic acid delivery, magnetofection is universally applicable to viral and nonviral vectors; because it is extraordinarily rapid, simple and yields saturation level transfection at low dose *in vitro* (Krotz *et al*., 2003). Further, since these magnetic particles do not rely on receptors or other cell membrane-bound proteins for cell uptake, it is possible to transfect cells that normally are non-permissive (Scherer *et al*., 2002).

1.8 TAILORING MAGNETIC NANOPARTICLES

1.8.1 Essential requisites

Magnetic nanoparticles for biological applications must be endowed with the specific characteristics required. The first requirement is often super paramagnetism. Super paramagnetism occurs in magnetic materials composed of very small crystallites (threshold sizes depends on the nature of the material, for instance, iron-based nanoparticles become super paramagnetic at sizes <25nm) (Lee *et al.,* 1996). In a paramagnetic material, the thermal energy overcomes the coupling forces between neighboring atoms above the Curie temperature (T_c) causing random fluctuations in the magnetization direction that result in a null overall magnetic moment. However in super paramagnetic materials, the fluctuations affect the direction of magnetization of entire crystallites. When the external magnetic field strength is applied, instead of each individual atom being independently influenced by an external magnetic field strength, the magnetic moment of entire crystallites aligns with the magnetic field strength.

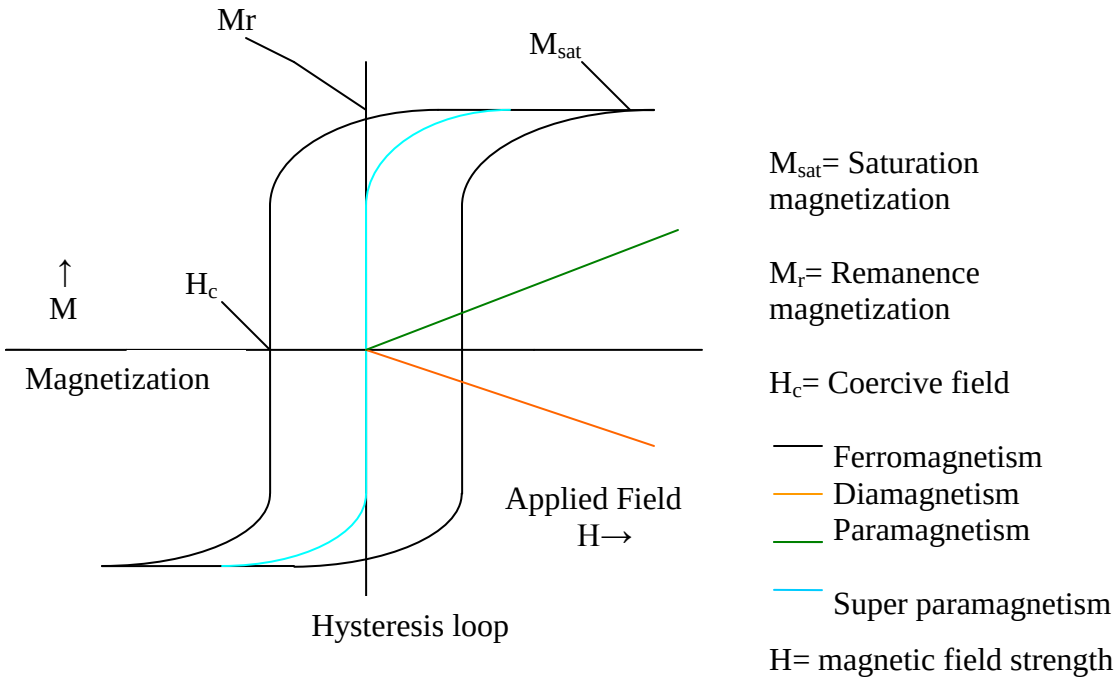

Figure. 6. Hysteresis loops (magnetization versus applied magnetic field strength) characteristic of ferromagnetic and super paramagnetic nanoparticles.

In large nanoparticles, energetic considerations favor the formation of domain walls. However, when the particle size decreases below a certain value, the formation of domain walls becomes unfavorable and each particle comprises a single domain. This is the case for super paramagnetic nanoparticles. Super paramagnetism in drug delivery is necessary because once the external magnetic field strength is removed, magnetization of the magnetic particles must disappear (negligible remanence and coercivity, see figure. 5), and so that agglomeration is avoided.

Another key requirement is the biodegradability or intact excretion of the magnetic core. Thus, super paramagnetic iron oxide nanoparticles are considered to be biodegradable with iron being reused/recycled by cells using normal biochemical pathways for iron metabolism (Bulte and Kraitchman, 2004).

1.8.2 Coatings on magnetic nanoparticles

Surface coatings of nanoparticles with various materials to form core-shell morphologies results in the formation of materials that can be used for the development of catalysts and optic-electronic devices (Ferrari, 2005; Cunningham *et al.*, 2005; Johannsen *et al.*, 2005). Studies on protective layer-coated ferromagnetic nanoparticles are of great interest for both fundamental magnetic investigations and practical engineering applications. In fundamental studies the coating on nanoparticles is of interest as it can prevent the nanoparticles from coarsening, surface oxidation, and agglomeration; in clinical applications, the coating protects the nanoparticles from leaching in an acidic environment; in soft magnetic applications, the coating not only works as an insulative phase to achieve high electric resistivity, but also behaves as a binder to ease the consolidation of the nanoparticles (Jurgons *et al.*, 2006; Jemal, 2007).

The coatings on magnetic nanoparticles often serve multiple purposes. Their role in reducing leaching of the cores has already been mentioned. Often coating also facilitates the stabilization of nanoparticles in an environment with a slightly alkaline pH or a significant salt concentration. For instance, the isoelectrical point of silicon dioxide (SiO_2) is reached at pH 2-3, meaning that silica-coated nanoparticles are negatively charged at the pH of blood, inducing electrostatic repulsion that helps avoid aggregate formation. Silica coatings also have additional advantages. The external surface of Silica coatings can be functionalized to allow the binding of biomolecules. This is mainly related to the presence of hydroxyl surface groups in significant concentrations that provide intrinsic hydrophilicity and allow surface attachment by covalent linkage of specific biomolecules (Ambrose and Fritz, 1998).

A variety of approaches have been developed to coat magnetic nanoparticles, including *in situ* coatings and post synthesis coatings. In the *in situ* coating approach, the magnetic nanoparticles are coated during the synthesis process. For example, Josephson and co-workers (Sunderland *et al.*, 2006; Neuberger *et al.*, 2005) have developed a co-precipitation process in the presence of the polysaccharide dextran. The coating is further cross linked chemically to increase the stability. This particular coating approach has

been very successful in producing dextran super paramagnetic iron oxide nanoparticles which are biocompatible and water-soluble, and can be used for a range of preclinical and clinical imaging studies. Other coatings in this class include a starch-based coating (Häfeli, 2004) and dendrimer coating (Widder *et al.*, 1981; Rotariu and Strachani, 2005).

The post-synthesis coating methods used for magnetic nanoparticles use a variety of materials, including monolayer ligands (Iacob *et al.*, 2004; Yellen *et al.*, 2005), polymers (Yellen *et al.*, 2005; Pankhurst *et al.*, 2003), combinations of polymers and biomolecules such as phospholipids and carbohydrates (Fréchet, 2005; Lübbe *et al.*, 2001), and silica coatings (Lübbe *et al.*, 1999; Lee *et al.*, 1996). Most monolayer coatings have low colloidal stability and because of toxicity of the capping ligands, limited application in medical imaging. The polymer and silica based coating process are difficult to control, often resulting in multilayered coatings and multiple nanoparticles in the same encapsulation (Lübbe *et al.*, 1999).

1.8.3 The fate of nanoparticles after administration into the body

The distribution of nanoparticles and their loads throughout the body depends on numerous physicochemical factors: size of particles, toxicity, surface charge, capacity for protein adsorption, surface hydrophobicity, drug loading and release kinetics, stability, degeneration of carrier system, hydration behavior, electrophoretic mobility, porosity, specific characteristics, density, crystallinity, contact angle, and molecular weight (Neuberger *et al.*, 2005). Nevertheless, the fate (and also the possible toxicity) of magnetic nanoparticles also depends strongly on the dose and administration route.

1.8.4 The toxicity of nanoparticles

When discussing the toxicity of nanoparticles, generalization becomes difficult because their toxicity depends on numerous factors including the dose, chemical composition, method of administration, size, biodistribution, surface chemistry, shape, and structure, to name but a few. With nanoparticles, as with any new biomedical discovery, the risk – benefit trade-off must be considered to assess whether the risks can be justified. In general, the size, surface area, composition, and coating of a nanoparticles are the most

important characteristics regarding cytotoxicity (Macaroff *et al.,* 2006), and modifications of the nanoparticles surface are a key tool to minimize toxicological effects (Park *et al.,* 2006).

It is well documented that the large surface-to-volume ratio of all nanosized particles can potentially lead to unfavorable biological responses if they are inhaled and subsequently absorbed via the lung or swallowed and then absorbed across the gastro intestinal tract (Duncan and Izzo, 2005). Interestingly, it has also been reported that in 20-100 mg/mL concentration, large magnetic particles show higher cytotoxicity than smaller ones even after normalizing for surface area (Yin et al., 2005) despite the lower surface-to-volume ratio, although it is difficult to perform comparable experiments with differently sized particles. In any case, toxicity studies should consider not only acute toxicity but also that of degradation products, the possible stimulation of cells with subsequent release of inflammatory mediators (Neuberger et al., 2005), and long-term toxicity.

1.9 OBJECTIVES OF THE RESEARCH

(a) To synthesize iron and iron oxide core-gold shell nanoparticles using two methods: micro emulsion (reverse micelle) and co-precipitation methods.

(b) To immobilise the iron and iron oxide core into gold shell materials or to grow the gold shell onto the magnetic seeds.

(c) To characterize the prepared particles using ultraviolet/visible spectroscopy, x-ray diffraction, transmission electron microscope and magnetization measurements.

(d) To compare the two synthesis methods in terms of nanoparticle stability.

1.9.1 THE STUDY PROBLEM (PROBLEM STATEMENT)

The nature of the problem to be investigated is:

Interest in core shell nanoparticles derives from the wide range of applications and the growing number of potential applications of such materials. This project is about the synthesis and characterizations of magnetic nanoparticles with a magnetic core and a gold shell. Magnetic nanoparticles have many technological applications. In particular they play an important role for data storage in modern information technology. Magnetic nanoparticles are studied because of their potential magnetic carriers for various biomedical uses such as cell and deoxyribonucleic acid separation, drug delivery system, magnetic resonance contrast enhancement and Gene cloning. There is sufficient motivation to explore several configurations of this simple core-shell modality, including the following: (1) the basic one core and a thin layered shell, (2) several core-shell layers and (3) a core-shell structure with a magnetic core and a composite layer containing smaller magnetic cores. The project is also about the immobilization of bio-compatible and/or bio-sensitive materials on such nanoparticles and the characterization of such immobilization. As a result of their potential for application in photodynamic therapy against cancer, applications in light harvesting devices and in electrochemical detection and quantitative analysis of a wide range of biological substrates (Sehlotho et al., 2006), the materials that have been identified for immobilization on these core-shell nanoparticles for this project are porphyrins and phthalocyanines. Immobilization of bio-materials such as specific antibodies and chemokine core-receptors and core-receptor ligands such as Chemokine (C-C motif) ligand 3 (CCL3) may be explored in the future (Seisdedos and Parmentier, 2006). The immobilization of substrate specific ligands on the surface of nanoparticles can also be used for the detection of substrates in mixtures (Zhang et al., 2007). The immobilization of antibodies on the surface of nanoparticles can be used for the detection of specific antigens (Aurich et al., 2007; Liu et al., 2006).

CHAPTER 2

EXPERIMENTAL

2.0 BACKGROUND

A number of methods have been developed by various workers in the preparation of super paramagnetic iron oxide nanoparticles (Chin and Yacoob, 2007; Kim *et al.,* 2008; Seino *et al.,* 2005; Guzman *et al.,* 2008; Kim *et al.,* 2001; Presa *et al.,* 2007; Maity *et al.,* 2009; Carvell *et al.,* 2009; Kinoshita *et al.,* 2003; Pham *et al.,* 2008) and perhaps the most recent is by Guzman *et al.,* 2008; Kim *et al.,* 2008; Carvell *et al.,* 2009 and Maity *et al.,* 2009.

The present work attempted to examine these various methods with the aim of preparing a super paramagnetic iron oxide nanoparticles combining or adopting methods from the various works earlier done.

A success was recorded in the use of citrate and cetyltrimethylammonium bromide (CTAB) as the surfactants.

2.1 THE CO-PRECIPITATION METHOD

2.1.1 MATERIALS AND METHODS

2.1.2 MATERIALS

Ferric (III) chloride hexahydrate ($FeCl_3.6H_2O$, >99%), Ferrous (II) chloride tetrahydrate ($FeCl_2.4H_2O$, >99%), Hydrogen tetrachloroaurate III hydrate ($HAuCl_4$), sodium citrate tribasic dihydrate ($Na_3C_6H_5O_7.2H_2O$, >99%), ammonium hydroxide (NH_4OH) were obtained from sigma-aldrich. The other chemicals were of analytical grade from other local suppliers and used without further purifications. All aqueous solutions were prepared using Millipore purified water (18.2 $M.\Omega cm^{-1}$). All the water used in experiments was deionized water (18.2 $M\Omega\ cm^{-1}$, Millipore Synergy 185).

2.1.3 METHOD

2.1.3.1 Preparation of reagents: $FeCl_3.6H_2O$ (17 mmol); $FeCl_2.4H_2O$ (8.5 mmol); NH_4OH (1M).

2.1.3.2 Synthesis of magnetite particles

Magnetite particles were prepared following the method reported by Liu *et al.* (2004). This method was slightly modified as detailed below

STEP I

Synthesis of the suspension of super paramagnetic iron oxide nanoparticles

Distilled deionised water and a mixture of ammonium hydroxide and sodium citrate dihydrate were deoxygenated by bubbling with pure nitrogen gas for 1 hour prior to use. Solutions of ferric (III) chloride hexahydrate, >99% and ferrous (II) chloride tetrahydrate, >99% were prepared as iron species with molar ratio 2:1

Procedure

Ferric (III) chloride hexahydrate (4.64g, 17 mmol) and ferrous (II) chloride tetrahydrate (1.71g 8.5 mmol) was dissolved in 250 mL deoxygenated water. To this vigorously stirred and nitrogen atmosphere-protected solution, a mixture of freshly deoxygenated ammonium hydroxide (1M, 100 mL) and sodium citrate dihydrate (1M, 19 mL) was added at a rate of 4 mL/min, resulting in a pale yellow color solution changing to brown and finally to dark black. After that, stirring was allowed for an additional 30 minutes, and the solution was then cooled to room temperature. This procedure is illustrated schematically in figure 6.

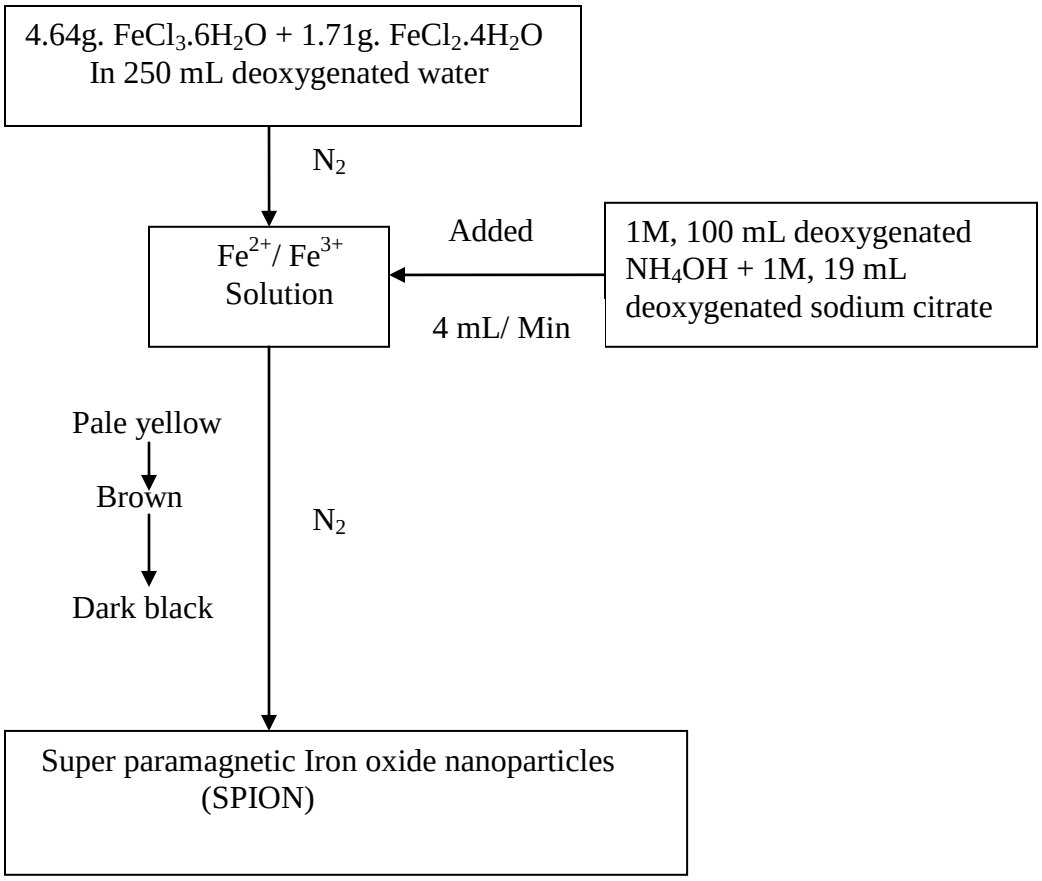

Figure. 7. Schematic diagram showing the procedures of forming the super paramagnetic Iron oxide nanoparticles.

STEP II

The gold coating process was as follows

As-synthesized suspension of super paramagnetic iron oxide nanoparticles (1.2 mL) was transferred into 200 mL deionized water. After addition of sodium citrate dihydrate (155.2 mM, 0.7 mL), this mixture was then stirred vigorously and heated to boil (98°C). During this period, magnetite particles would be oxidized partially or completely to maghemite before their being coated (Lyon *et al.*, 2004; Tang *et al.*, 2003). Once boiling, hydrogen tetrachloroaurate (III) hydrate solution (10 mM, 10 mL) was injected as soon as possible, and the initially pale yellow solution changed color to brown and dark brown, and then to final deep red characteristic gold colloids. The heating mantle was removed

15 minutes after injection, and the stirring was continued for an additional 15 minutes. This procedure is illustrated schematically in fig. 7.

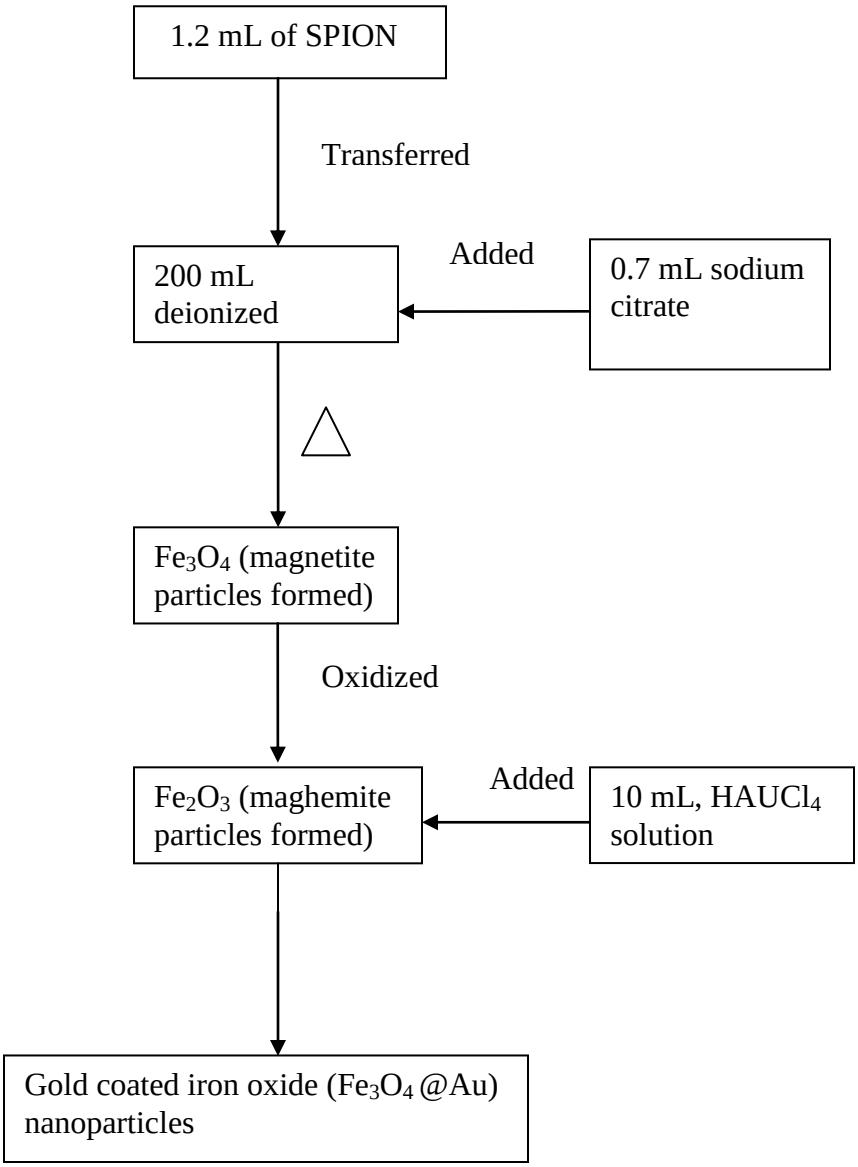

Figure. 8. Schematic diagram showing the procedures of coating the iron oxide nanoparticles with gold and the formation of magnetic nanoparticles (magnetite@gold nanoparticles).

2.2 THE REVERSE MICELLE (MICROEMULSION) METHOD

The reverse micelle reaction is carried out using cetyltrimethylammonium bromide a as the surfactant, octane as the oil phase, and aqueous reactants as the water phase. Varying the water to surfactant ratio (w) can form micelles ranging in size from 5 to 30 nm thus leading to careful control over the particle size. A co-surfactant of n-butanol is used to help decrease the fraction of the micellar head group that is neutralized and thereby increase the stability of the micelle. Without the addition of the co-surfactant, the amount of free water available to carry on the reactions is greatly reduced, as most of the water is locked in the head group of the cetyltrimethylammonium bromide.

The metal Ps is formed inside the reverse micelle by the reduction of a metal salt using sodium borohydride ($NaBH_4$). The sequential synthesis offered by reverse micelles is utilized to first prepare an iron core by the reduction of ferrous sulfate ($FeSO_4$) by sodium borohydride. After the reaction has been allowed to go to completion, the micelles within the reaction mixture are expanded to accommodate the shell using a larger micelle containing and additional sodium borohydride. The shell is formed using an aqueous hydrogen tetrachloroaurate (III) hydrate solution. This procedure is illustrated schematically in fig. 8.

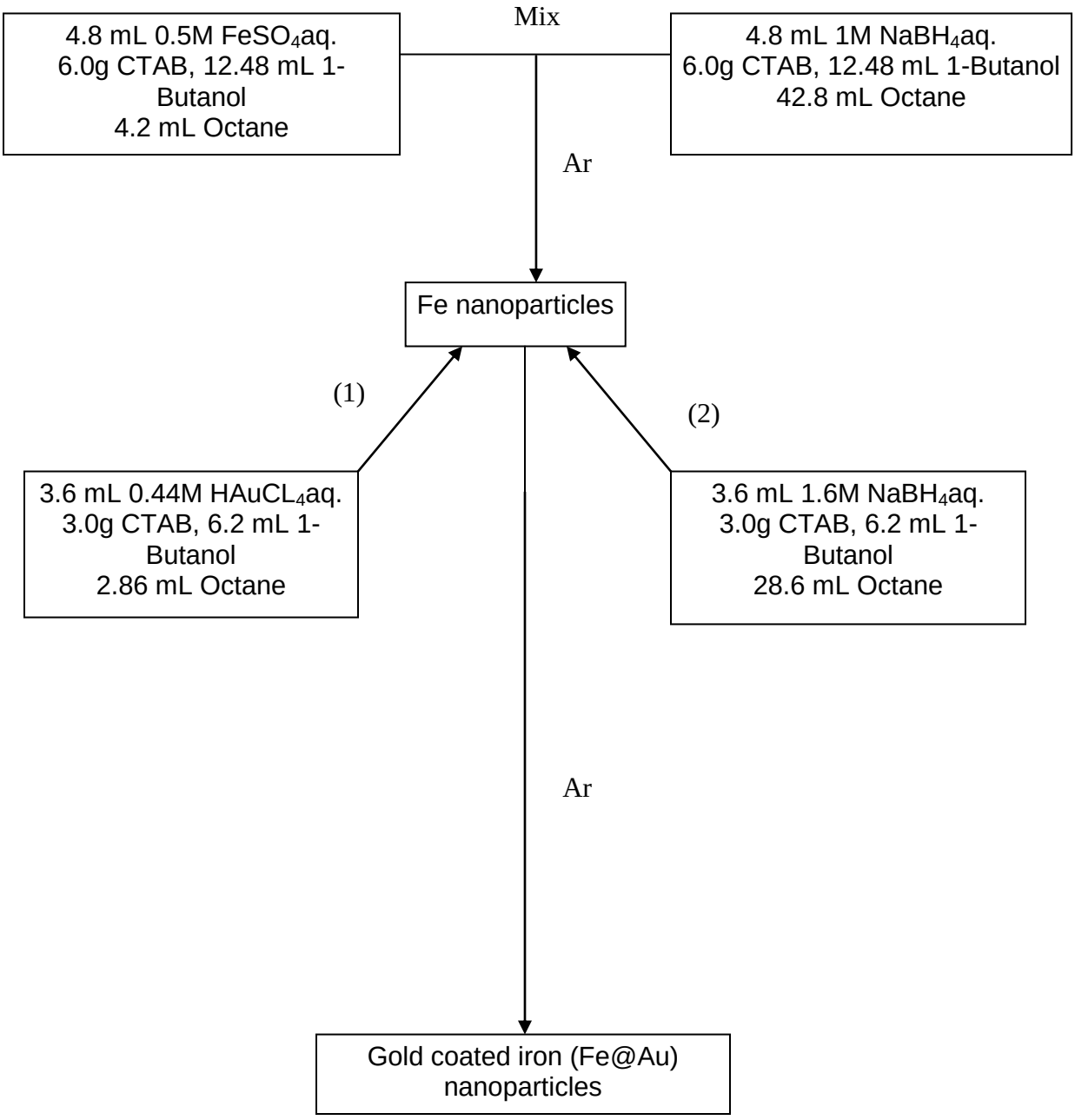

Figure. 9. Schematic diagram showing the procedures of forming the iron@gold nanoparticles

2.2.1 Sample Preparation

Gold-coated iron nanoparticles (Fe@Au) were prepared following the method reported by Pana *et al.* (2007). This method was slightly modified as detailed below. Gold-coated iron nanoparticles were generally obtained by reverse micelle method. We used ferrous sulfate ($FeSO_4.7H_2O$) and hydrogen tetrachloroaurate (III) hydrate as precursors and sodium borohydride as reducing agent; $FeSO_4$ (4.8 mL, 0.5 M) (aq.), CTAB (6 g), 1-butanol (12.48 mL), octane (42.8 mL) were mixed up with $NaBH_4$ (4.8 mL, 1M), CTAB (6 g), 1-butanol (12.48 mL) and octane (42.8 ml). This mixture was stirred for 1 h, at room temperature under inert atmosphere.

Another mixture containing $NaBH_4$ (3.6 mL 1.6M) + CTAB (6 g) + 1-butanol (6.2 mL) + octane (28.6 mL) and $HAuCl_4$ (3.6 mL, 0.44M) + CTAB (3g) + 1-butanol (6.2 mL) + octane (2.86 mL) was added into the solution, after 1 hour.

The new solution was stirred for 5 hours, at the room temperature under inert atmosphere. In this synthesis the cetyltrimethylammonium bromide was the surfactant and the 1-butanol was the core-surfactant. After synthesis, the remaining surfactants were removed by thorough washing with a 1:1 chloroform/methanol mixture and the resulting magnetic nanoparticles were dried in an oven at 40^oC for 1day.

2.3 Characterizations

Transmission electron microscope measurement was done with Hitachi 8000 accelerating the voltage at 200 kV ultrahigh resolution analytical electron microscopes. Transmission electron microscope was used to measure the morphology and size of samples obtained. The samples for transmission electron microscope analyses were obtained by diluting the dispersed solution with ethanol and then placing a drop of the diluted solution onto a covered copper grid and evaporated in air at room temperature. Before the samples were withdrawn, the nanocomposites dispersed ethanol solutions were sonicated for 5 minutes to obtain the better particles dispersion on the copper grid.

Vibrating sample magnetometer (VSM, EG & G Princeton Applied Research Vibration Sample Magnetometer, Model 155) was used to investigate the magnetic properties of nanocomposites by measuring the magnetization as a function of magnetic field strength intensity.

The temperature dependence of magnetization of iron nanocomposites was investigated by a superconducting quantum interference device (SQUID) magnetometer (MPMS5, Quantum Design) at a temperature ranging from 2 to 300 K under different applied magnetic field. Weighed amount of samples were packed in gel capsules and placed tightly in the glass tube ensuring no movement in either direction and the magnetic properties were measured.

An x-ray diffraction (D8 FOCUS 2.2 kW, Bruker, Germany) was used to characterize magnetite nanopowder and gold-iron oxide nanoparticles, respectively. The x-ray diffraction patterns were taken from 20 to 80˚ (2θ value) using CuKα radiation with an intensity ratio (α_2/α_1) = 0.5 and wavelengths of 1.54439 and 1.54056 Å, respectively.

UV-visible spectra were measured with a Hewlett-Packard 8452A Diode-Array spectrophotometer.

CHAPTER 3

3. RESULTS AND DISCUSSIONS

3.1 THE CO-PRECIPITATION METHOD

3.1.1 Structural analysis of magnetic cores by X-ray diffraction

Fig.10 illustrates the x-ray diffraction pattern of synthesized magnetite nanoparticles in alkaline solution. The pattern of magnetite nanoparticles is face-centered cubic (FCC), a=8.39Å and special group $Fd\bar{3}m$ (227); the dominant crystal plane is 311.The stabilizing agent of oxidized magnetite was exchanged to citrate ions to facilitate the reduction of Au^{3+} on the surface using sodium citrate as reducing agent.

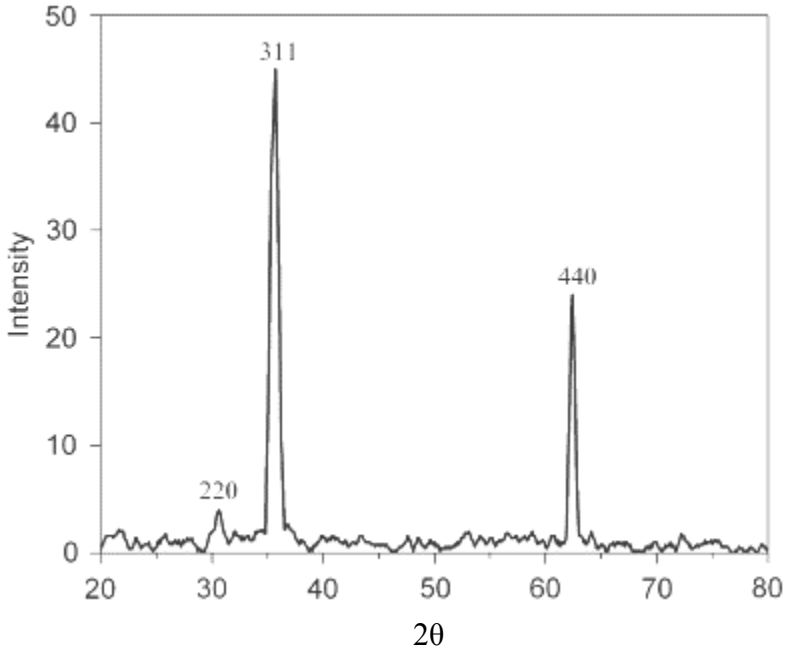

Figure. 10. X-ray diffraction pattern of magnetite nanoparticles.

3.1.2 Structural analysis of gold-iron oxide nanoparticles

To form the gold shell, gold precursor ions were directly added to a boiling solution of both sodium citrate and oxidized magnetite cores, following the sodium citrate seeding method on gold nanoparticles of Brown and Natan (Brown *et al.*, 2000; Lu *et al.*, 2006).

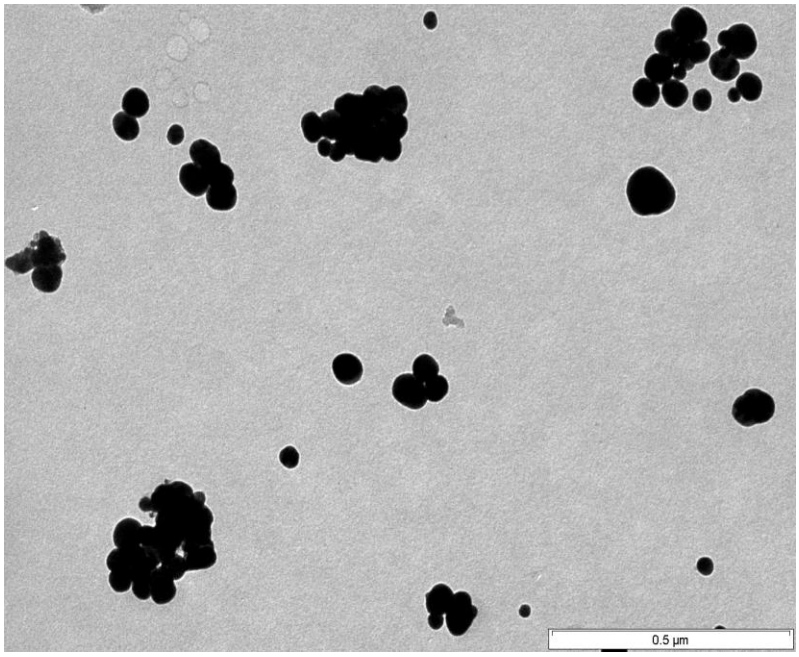

Figure. 11. Transmission electron microscope image of the as-prepared nanoparticles, scale bar: 0.5 µm

Fig. 11 displays the representative transmission electron microscope image of these gold-iron oxide nanoparticles. These gold-iron oxide nanoparticles were separated from gold nanoparticles by a magnet. The jagged appearance is likely due to the initial reduction of Au^{3+} at specific sites on the surface of face-centered cubic iron oxide particles whereas spherical surfaces of Au^{3+} results from further reduction. Herein, the size distribution of gold-iron oxide nanoparticles is 0.5 µm=500 nm. An excessive concentration of sodium citrate was used to reduce the Au^{3+} ions on the surface of the magnetic cores.

The creation of the core/shell structure by the hydroxylamine seeding method was expected to reduce gold ions on the surface of the oxidized magnetite. However, the

reduction of precursor gold ions resulted in both the formation of gold shell onto iron oxide and the formation of gold nanoparticles (Lyon *et al.,* 2004). In this experiment, Au^{3+} ions were reduced by 1 M sodium citrate in solution. Further, Au^{3+} ions could not be reduced to form the gold shell on iron oxide cores when sodium borohydride was used as the sole reducing agent to make the gold shell without exchanging ammonium hydroxide with citrate ions, indicating that the presence of citrate ions before the reduction occurs plays a key role. The elemental mapping performed by transmission electron microscope imaging supports the confirmation of both gold and iron in one representative nanoparticle (Inset 1).

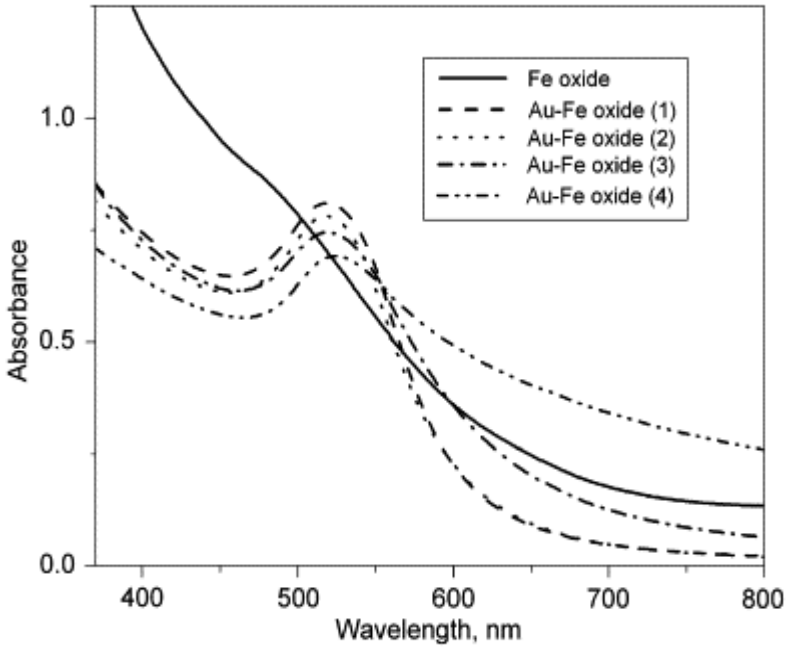

Figure. 12. Absorption spectra of gold-iron oxide nanoparticles solutions with different ratio between concentration of Au^{3+} ions and concentration of iron oxide (the ratio decreases from 1 to 4).

Gold nanoparticles have strong surface plasmon giving an absorption peak in the visible region of the electromagnetic spectrum. In particular, it has been reported that citrate stabilized gold nanoparticles in water exhibited a surface plasmon peak at 520 nm (Brown *et al.,* 2000). Spectra of the composite nanoparticles prepared herein with various ratios of Au^{3+} to iron oxide were collected and are shown in figure 12. There were no

significant absorption peaks attributable to iron in the visible region of the spectra of the pure iron oxide solution while the surface plasmon peaks appeared in the range of 500-700 nm of the gold-iron oxide solutions, indicating the formation of gold shell or/and gold nanoparticles. As the ratio of Au^{3+} to iron oxides decreased from 1 to 4, the surface plasmon peak blue-shifted far away from the expected peak of pure citrate-stabilized gold nanoparticles. In addition, the sharpness of the peak was reduced together with the breadth of the band as the ratio decreased. The presence of different iron oxide core may affect the surface plasmon peak, resulting in induced electron properties of the particles (Lyon *et al.*, 2004). The various peak extensions may also be caused by non-uniform gold shells around the iron oxide cores. The higher concentration of iron oxide cores is likely to cause the formation of bigger gold-iron oxide particles, which in turn results in formation of broader surface plasmon bands since larger particle diameters lead to increasing ellipticities and to significantly broadening of the optical spectra.

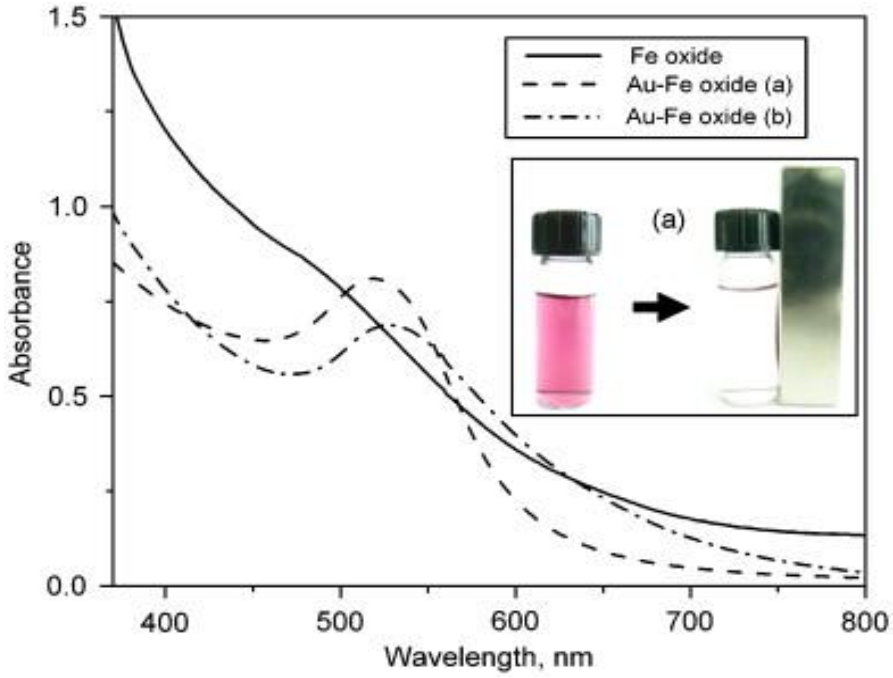

Figure. 13. Absorption spectrum of pure gold-iron oxide nanoparticle solution separated by magnet (b) compared with that of the solution containing both gold-iron oxide nanoparticles and gold nanoparticles. Inset (a) describes the pure gold-iron oxide nanoparticles entirely separated by a magnet.

Gold-iron oxide nanoparticles were separated from gold nanoparticles by using a 3000 G magnet as illustrated in inset (a) of Fig.13. The results show different magnetization of gold-iron oxide nanoparticles. The difference in magnetization may be derived from the different magnetic cores and size of gold-iron oxide nanoparticles. Further, the concentration of sodium citrate as the reducing agent in our study is much higher, indicating that high concentration of citrate ions may facilitate the reduction of gold on the surface of iron oxides. In this study, partially oxidized magnetite synthesized in 1M ammonium hydroxide solution was used as magnetic cores. After magnetic separation, the gold-iron oxide nanoparticles were still well dispersed in aqueous solutions. The pure gold-iron oxide nanoparticle solution had a surface plasmon peak at a higher wavelength of 528 nm (line b), with a broader band compared to the non-separated gold-iron oxide solution (line a) as displayed in Fig.13. Furthermore, gold-iron oxide nanoparticles fabricated by the hydroxylamine seeding method were not separated from pure gold nanoparticles (Lyon *et al.,* 2004), showing a surface plasmon resonance peak that blue-shifts from 570 to 525 nm. Hence, gold-iron oxide nanoparticles prepared herein using sodium citrate as a sole reducing agent was separated from non magnetic particles using a magnet.

3.1.3 Magnetic measurements of the nanocomposite

When a sample is cooled in zero fields (ZF), the total magnetization will be zero since the magnetic moments of the particles are randomly oriented. The application of magnetic field strength, however, induces a net magnetic moment along the field direction, which will increase temperature as more and more particles orients their magnetic moments parallel to the field. At the temperature at which the relaxation time of most of the magnetic moments of particles equal the experimental resolution time, the zero-field-cooled curve comes to a maximum, which corresponds to the case when the majority of the particles behave superparamagnetically. This temperature is the blocking temperature. At temperature higher than blocking temperature, the magnetization decreases, as shown in Fig.14. If the samples are cooled in the presence of a magnetic field strength to generate the field-cooled curve, both the field-cooled and zero-field-cooled curves coincide until they come to blocking temperature (equilibrium magnetization). Below blocking temperature, the field-cooled curve splits from the zero-field-cooled curve, since it does not correspond to the equilibrium. Moreover, the zero-field-cooled curve relaxes toward the field-cooled curve. That is, below blocking temperature, blocking of the magnetic moments occurs for times longer than the experimental resolution time. There are metastable states separated by energy barriers, which prevent free magnetization reversal, and both relaxation and hysteresis phenomenon are observed. For the sample magnetite, field-cooled magnetization curve increases very slowly with decreasing temperature and tend to flatten off. Its temperature behavior is definitely different from the $1/T$ Curie-like law expected for no interacting particles and suggests the presence of interparticle interactions, presumably of the dipole-dipole type (Del Barco *et al.,* 2001). For all other samples from magnetization 2 to magnetization 4 the nature of the field-cooled and zero-field-cooled curves remains the same with the change of blocking temperature. The blocking temperature for magnetization 1, magnetization 2, magnetization 3, and magnetization 4 are 150, 143, 138, and 135 K, respectively. Hence blocking temperature decreases with the increase of the thickness of the gold shell (Fu *et al.,* 2001). This happens because the layer covers each individual nanoparticle and the interparticle separation increases, thus reducing the magnetic dipole-dipole interaction.

This lead to a shift in blocking temperature for coated particles. So increasing the thickness of the coating pushes the blocking temperature to lower temperatures.

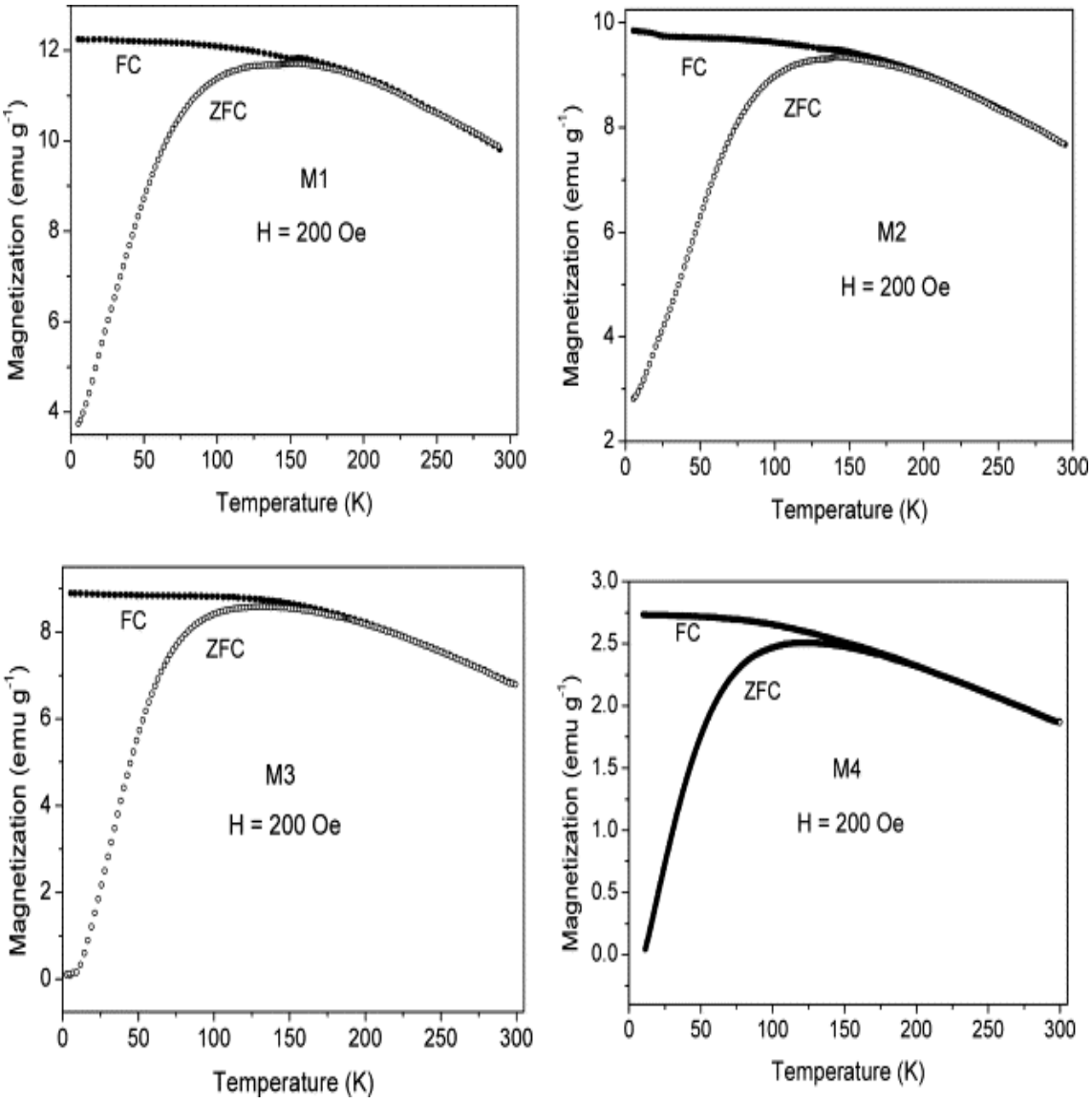

Figure. 14. Magnetization vs. temperature {[Zero-Field-Cooled (ZFC)]} and {[Field-Cooled (FC)]} plot of samples, magnetization 2, magnetization 3, and magnetization 4: [$HAuCl_4$] molar ratios are 1:0.1, 1:0.5, and 1:1, respectively.

The plots of magnetization vs magnetic field strength (magnetization-magnetic field strength-loop) at room temperature and 10 K for the typical magnetic nanoparticles without (magnetization 1) and with a coating of gold (magnetization 3) are shown in

Fig.15. At room temperature no hysteresis loop was obtained for the samples, but at 10 K a clear hysteresis revealed the resultant magnetic nanoparticles to be super paramagnetic in nature, and the particles were so small that they may be considered to have a single magnetic domain (Murakami *et al.,* 2002). Saturation magnetization of bulk magnetite is 92 emu/g (Zaitsev *et al.,* 1999), but here for these magnetite nanoparticles it is 38 emu/gm at room temperature. So it is reduced by 57.6% from the bulk. The reduction in saturation magnetization may be due to the increase in particle size.

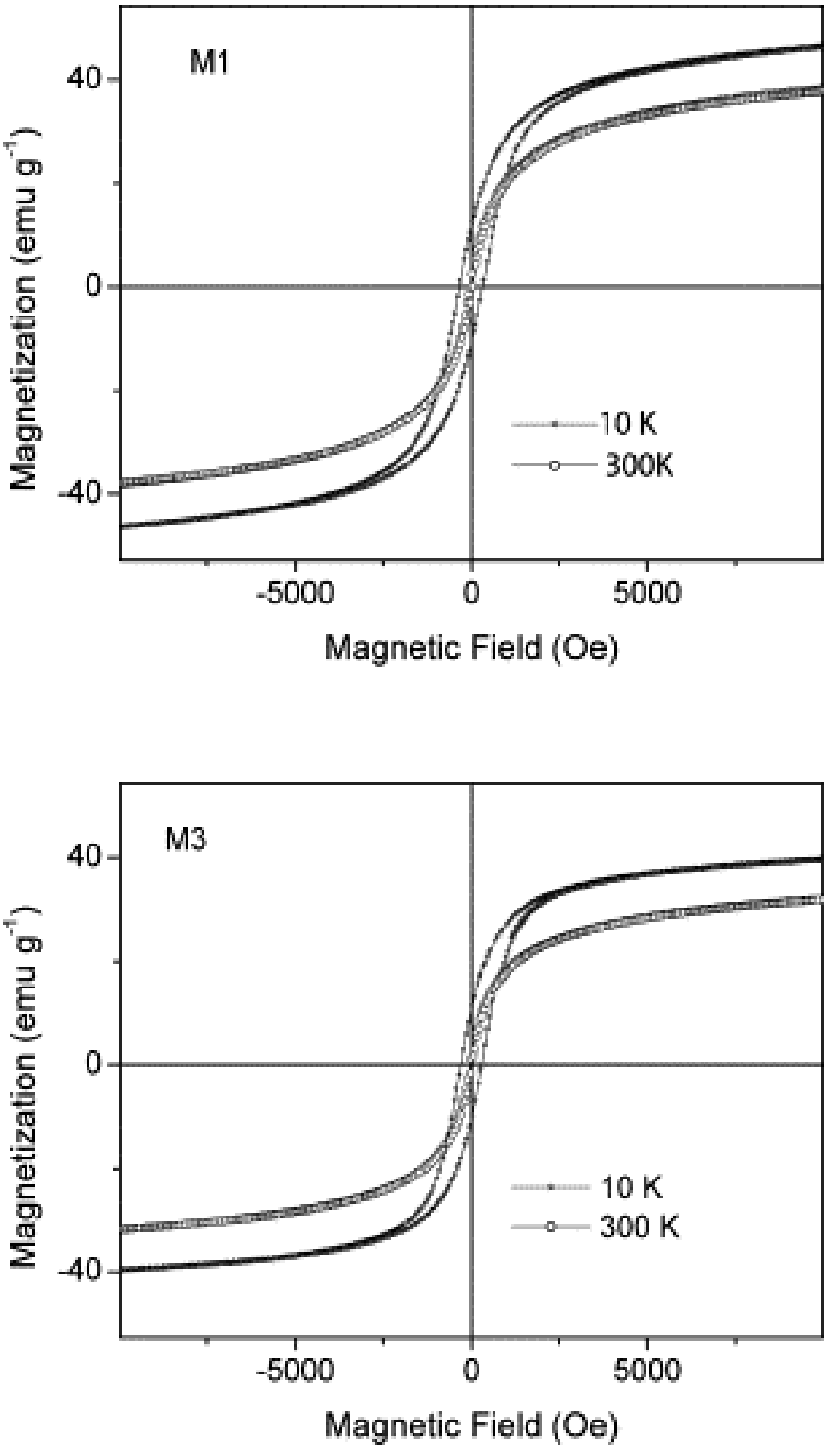

Figure. 15. Hysteresis curves for two samples, magnetization 1 and magnetization 3, at 10 K and at room temperature (298 K). Hydrogen tetrachloroaurate (III) hydrate molar ratio is 1:0:5.

3.2 THE REVERSE MICELLE (MICRO EMULSION) METHOD

3.2.1 Structural properties of X-ray diffraction

A representative x-ray diffraction pattern of the iron-gold nanoparticles is shown in Fig.16. All the peaks correspond to the face-cubic centered metallic gold diffraction. The pattern of α-iron is hidden under the pattern of gold due to the overlapping of their diffraction peaks at $2\theta = 44.8^{\circ}$, 65.3°, and 82.5°. Further evidence for the presence of iron in the sample is from the energy X-ray spectrum (EDS) (figure not shown for energy dispersive spectroscopy) attached with a transmission electron microscope, where the elements gold and iron have been found. Gold and iron are from the sample. No oxygen is detected in the energy dispersive spectroscopy and no diffraction patterns of iron oxide are observed in the x-ray diffraction, indicating that the iron nanoparticles are well protected by the gold shell.

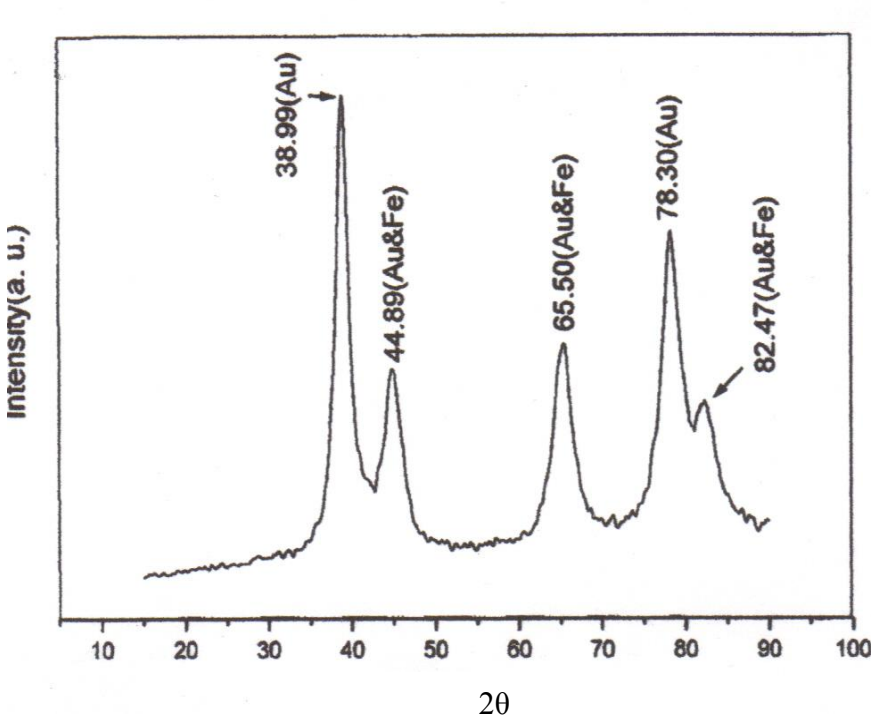

Figure. 16. X-ray diffraction pattern of the iron@gold nanoparticles.

3.2.2 Optical properties

The absorption spectrum of the colloid of iron@gold nanoparticles has been measured, which is compared with that of pure gold nanoparticle colloid prepared in the same way. The gold colloid shows a red color, while the iron@gold colloid displays a black-blue color. Fig. 17 shows the absorption spectra of the iron@gold colloid (a) and gold colloid (b). The gold colloid exhibits an absorption band with a maximum at 526 nm, while the iron@gold colloid shows an absorption band with a maximum at 555 nm. Furthermore, the latter is broader than the former. The absorption of metallic nanoparticle colloids such as gold, silver, etc. is due to the surface plasmon absorption (Taleb *et al.*, 1997). The red shift and broadening in the surface plasmon absorption of the iron@gold colloid relative to the pure gold colloid reveals that the size distribution of pure gold nanoparticles is narrower than that of the iron@gold nanoparticles and that there is aggregation of iron@gold nanoparticles.

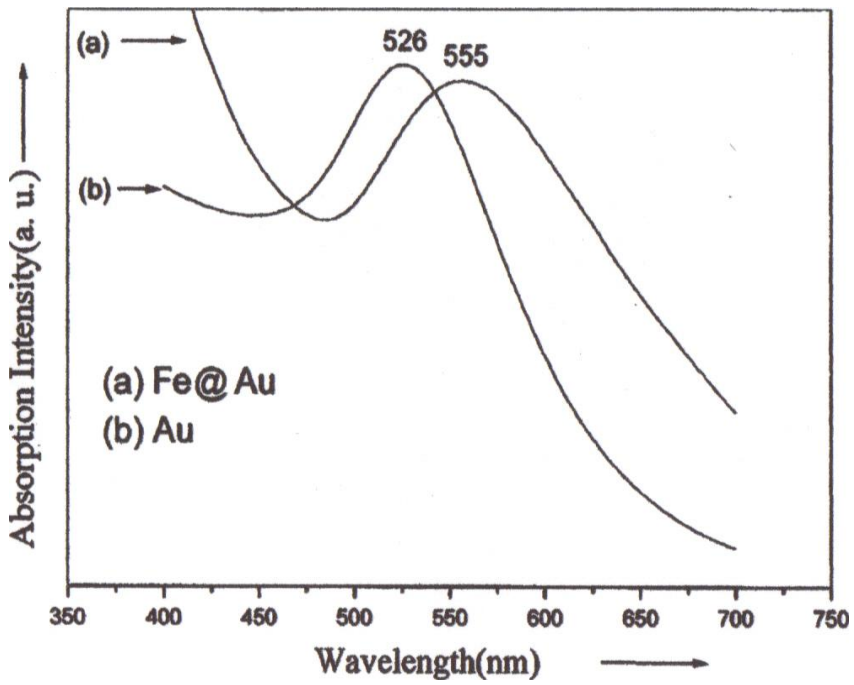

Figure. 17. Absorption spectra of the (a) iron@gold colloid and (b) gold colloid in toluene.

3.2.3 Magnetic properties

Magnetic properties of the dried iron@gold nanoparticles were derived from zero-field-cooled and field-cooled magnetization as a function of temperature and from magnetization vs magnetic field strength loops at 2, 10, and 300 K, respectively. The sample was initially cooled in a zero field to 2 K. A 1000 Oe field was then applied and magnetization was recorded as the temperature was increased (this is a zero-field-cooled curve). When the temperature reached 300 K, the sample was progressively cooled and the magnetization was recorded. This curve is called field-cooled. Fig.18 shows the zero-field-cooled/field-cooled curves. In the field-cooled curve (fig.18b), the magnetization nearly stays constant from 2 to 42 K and then shows a uniform decay as the temperature increases. A maximum magnetization can be observed in the zero-field-cooled curve (fig. 18a) at 42 K, indicating that the blocking temperature of iron@gold nanoparticles is 42 K. Below 42 K (blocking temperature), the particles are blocked and in a ferromagnetic state with an irreversible magnetization, whereas above blocking temperature, the magnetization is reversible and the particles are characterized by super paramagnetic behavior (Petit *et al.*, 1998). The shape of the zero-field-cooled curve also suggests a relatively narrower size distribution of the iron@gold nanoparticles (Waniewska *et al.*, 1992).

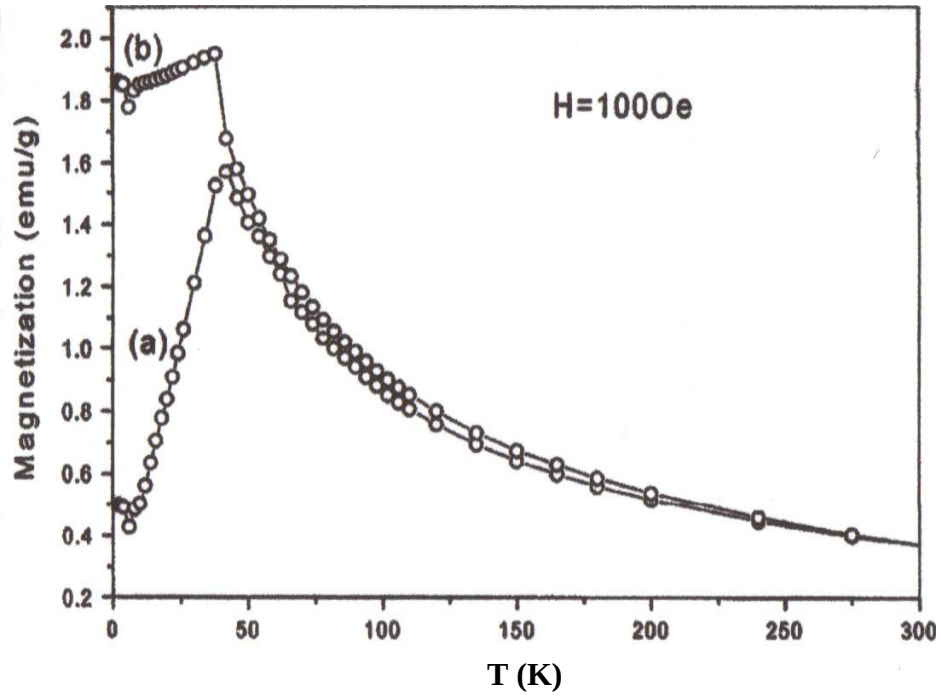

Figure. 18. Zero-field-cooled/ field-cooled curve of iron-gold nanoparticles: (a) Zero-field-cooled; (b) Field-cooled.

Figures 19a-19c illustrate the magnetization of iron@gold nanoparticles as the magnetic field strength of the susceptometer cycles between + 60 and − 60 kOe at 2, 10, and 300 K, respectively. Below the blocking temperature (42 K), the iron@gold nanoparticles are in a ferromagnetic state, showing a coercivity and remanence of 728 Oe and 4.12 emu/g at 2k (Fig. 19a) and 322 Oe and 2.92 emu/g at 10 K (Fig. 19b), respectively. Above the blocking temperature, in the super paramagnetic regime, no coercivity or remanence is observed at 300 K (Fig. 19c). (Carpenter *et al.,* 1999).

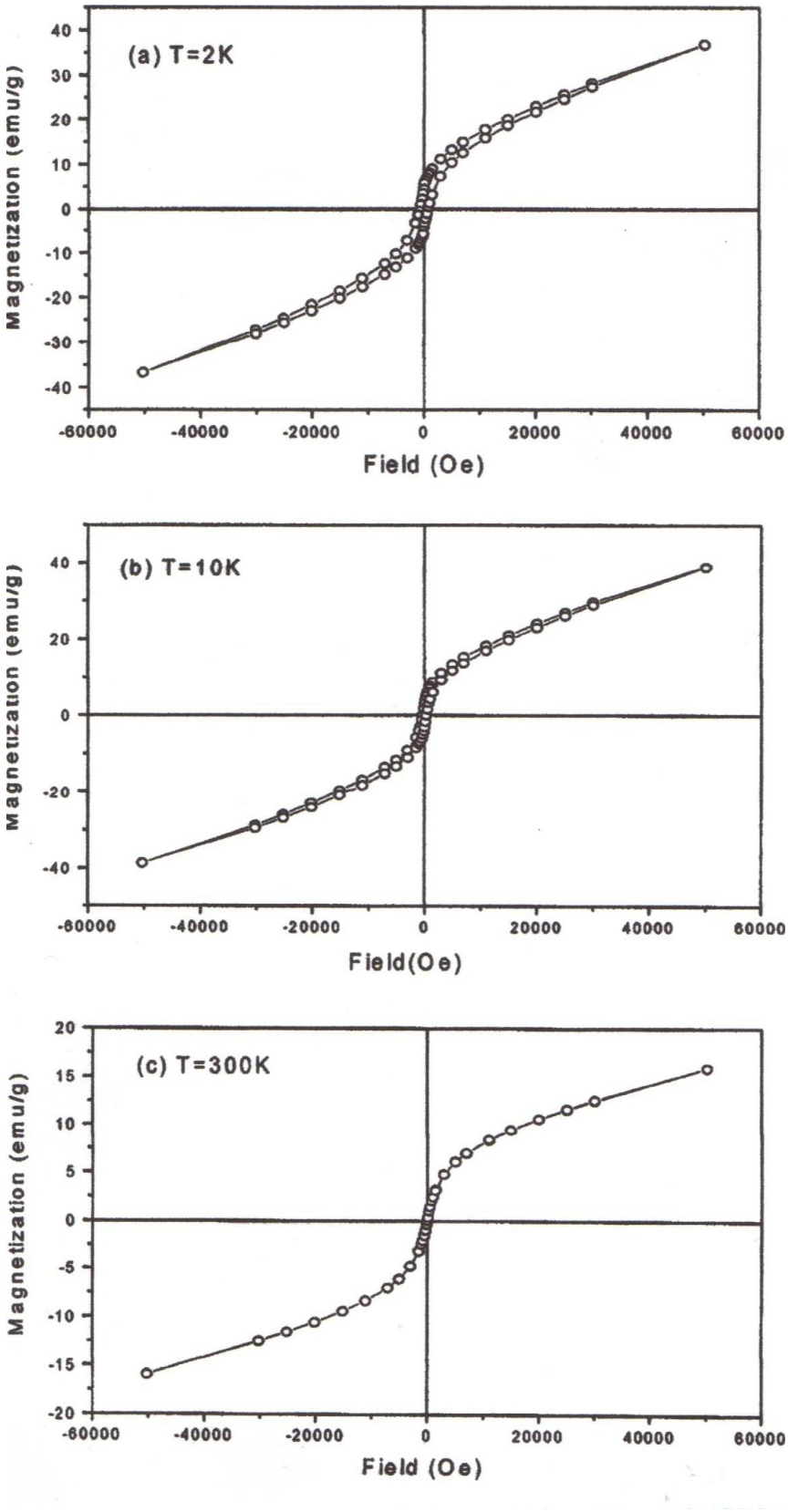

Fig. 19. Magnetization of iron@gold nanoparticles vs the magnetic field strength at 2K (a), 10K (b), and 300 K.

3.2.4 Self-assembling properties

Successful self-assembly of nanoparticles arrays depends on the ability to prepare monodisperse particles and to balance the interparticle forces so that ordered structures form spontaneously. Compared to other self-assembly systems, nanoparticles have an additional magnetostatic force, which favors the formation of magnetically aligned chains of magnetic dipoles, rather than two- or three-dimensional structures (Jin *et al.*, 1999).

This is actually the case for our iron@gold nanoparticles. The self-assembling of iron@gold nanoparticles was performed under a magnetic field strength (0.5 T) and checked by transmission electron microscope. Fig. 20 below shows the resulted transmission electron microscope micrograph. In the higher magnification micrograph (Fig. 20), a single iron@gold nanoparticle can be resolved clearly, with a size distribution of 2 μm=2000 nm.

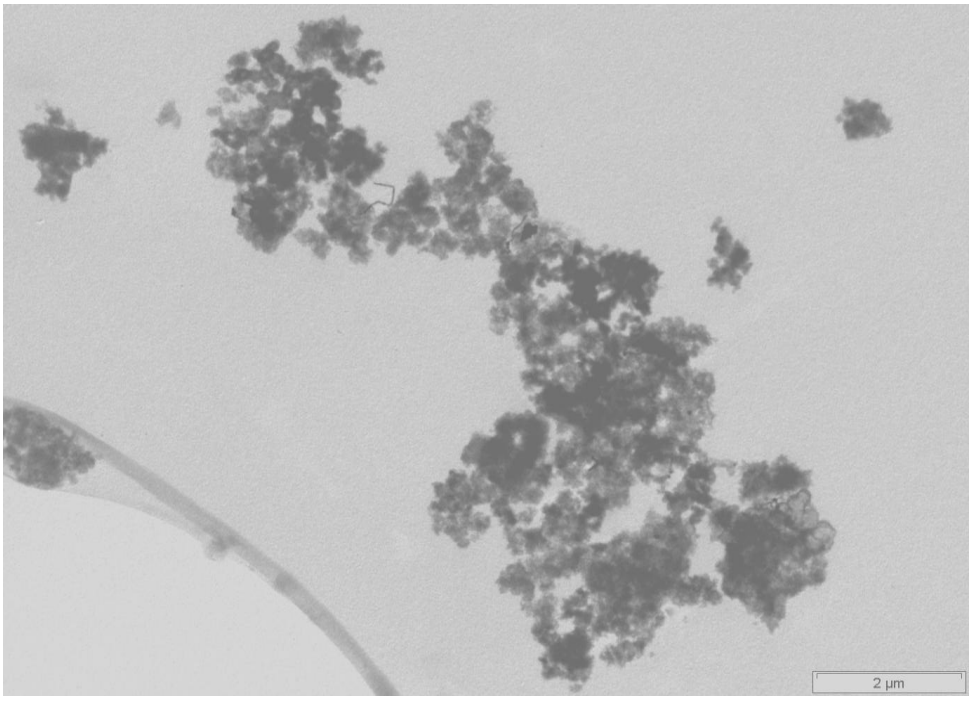

Figure. 20. Transmission electron microscope image of a sample of 2 μm iron@gold nanoparticles (dark spots) after synthesis. Lighter areas are the surfactant cetyltrimethylammonium bromide.

CHAPTER 4

CONCLUSION

The following conclusions can be drawn from this study:

4.1 The co-precipitation method

Magnetic composite nanoparticles consisting of magnetic iron oxide and gold were synthesized in an aqueous solution using a co-precipitation method. The x-ray diffraction patterns indicated that as-synthesized iron oxide nanoparticles were magnetite. According to the transmission electron microscope image, the particle size was around 500 nm, and the magnetite nanoparticles were spherical in shape. The iron oxide nanocomposites were stable and showed super paramagnetic characteristics with its saturation magnetization of 38 emu/g. Ultraviolet-visible absorption spectra of the composite nanoparticles showed surface plasmon peak of separated gold-iron oxide nanoparticles at 528 nm of nano-sized gold while the non-separated solution (containing gold nanoparticles) shows a peak at 520 nm. Further studies are needed to investigate chemical functionalization and immobilization of biological molecules on gold surface. Chemical reduction of gold (III) ions leads to the formation of gold nanoparticles in an aqueous phase, which are immobilized on the surface of magnetic nanoparticles. Thus a synthesized composite nanoparticle carries function of gold and magnetic iron oxides, so that it would be magnetic nanocarrier suitable for biomedical applications.

4.2 The reverse micelle (micro emulsion) method

Magnetite nanoparticles (iron@gold nanoparticles) were successfully produced at room temperature *via* w/o micro emulsion method (approach), which was characterized by x-ray diffraction, transmission electron microscope, ultraviolet/visible absorption spectra, and magnetic measurements. The x-ray diffraction pattern of α-iron is hidden under the pattern of gold. A red shift and broadening occurs in the absorption band of the iron@gold colloid compared with that of the pure gold colloid. The blocking temperature for iron@gold nanoparticles is 42 K, above which the particles are in a super

paramagnetic state and below which in a ferromagnetic state. The saturation magnetization and the coercivity of iron@gold nanopowders at 2 K were 4.12 emu/g and 728 Oe, and at 10 K were 2.92 emu/g and 322 Oe respectively. These iron@gold nanoparticles are self-assembled into chains on the micro scale under a magnetic field strength. According to the transmission electron microscope, the size distribution was found to be around 2 μm (2000 nm) and the particle shape was almost a sphere. The gold colloids exhibited an absorption band with a maximum peak at 526 nm, while the iron@gold colloid shows an absorption band with a maximum peak at 555 nm.

REFERENCES

Ashtari P., He X., Wang K. and Gong P. (2005). An efficient method for recovery of target ssDNA based on amino-modified silica-coated magnetic nanoparticles. Talanta, 67: 548-554.

Aurich K., Schwalbe M., Clement J.H., Weitschies W., and Buske N. (2007). Polyaspartate coated magnetic nanoparticles for biomedical applications. Journal of Magnetism and Magnetic Materials, 311: 1-5.

Ambrose D.L. and Fritz J.S. (1998). High-performance liquid chromatographic determination of drugs and metabolites in human serum and urine using direct injection and a unique molecular sieve. Journal of Chromatography B: Biomedical Sciences and Applications, 709: 89-96.

Arbab A.S., Bashaw L.A., Miller B.R., Jordan E.K., Lewis B.K., Kalish H. and Frank J.A. (2003). Characterization of biophysical and metabolic properties of cells labeled with superparamagnetic iron oxide nanoparticles and transfection agent for cellular MR imaging. Radiology, 229: 838-846.

Bailey R.L (1983). Lesser known applications of ferrofluids. Journal of Magnetism and Magnetic Materials, 39: 178-182. Journal of Magnetism and Magnetic Materials, 124: 228-238.

Batlle X., Obradors X., Medarde M., Carvajal J.R., Pernet M. and Rigi M.V. (1993). Surface spin canting in $BaFe_{12}O_{19}$ fine particles. Journal of Magnetism and Magnetic Materials, 124: 228-238.

Bean C.P. and Livingstone J.D. (1959). Superparamagnetism. Journal of Applied Physics, 30: 120S-129S.

Berry C.C. and Curtis A.S.G. (2003). Functionalisation of magnetic nanoparticles for applications in biomedicine. Journal of Physics D: Applied Physics, 36: R198-R206.

Berry C.C., Wells S., Charles S. and Curtis A.S.G. (2003). Dextran and albumin derivatised iron oxide nanoparticles: influents on fibroblasts in vitro. Biomaterials, 24: 4551-4557.

Boyd B.J. (2005). Technology overviews. Colloidal Drug Delivery, drug delivery report autumn/winter, PharmaVentures Ltd, Oxford, UK: 63.

Bradbury A., Menear S., O'Grady K. and Chantrell R.W. (1984). Magnetic size determination for interacting fine particle systems. Institute of Electrical and Electronics Engineers Transactions on Magnetics, 20: 1846-1848.

Brown K.R., Walter D.G. and Natan M.J. (2000). Seeding of colloidal Au nanoparticle solution. 2. Improved control of particle size and shape. Chemistry of Materials, 12: 306-313.

Bulte J.W.M. and Kraitchman D.L. (2004). Iron oxide MR contrast agents for molecular and cellular imaging. Nuclear Magnetic Resonance Biomedical, 17: 484-489.

Bulte J.W., Douglas T. and Witwer B. (2001). Magnetodendrimers allow endosomal magnetic labeling and in vivo tracking of stem cells. Nature Biotechnology, 19: 1141-1147.

Carpenter E.E. (2001). Iron nanoparticles as potential magnetic carriers. Journal of Magnetism and Magnetic Materials, 225: 17-20.

Carpenter E.E., Sangergorio C. and O'Connor C.J. (1999). Effects of shell thickness on blocking temperature of nanocomposites of metal particles with gold shell. Institute of Electrical and Electronics Engineers for Transmission Magnetism, 35: 3496-3498.

Carvell J., Ayieta E., Johnson M. and Cheng R. (2009). Characterization of iron nanoparticles synthesized by high pressure sputtering. Materials letters, 63: 715-717.

Chan D.C.F., Kirpotin D.B. and Bunn Jr P.A. (1993). Synthesis and evaluation of colloidal magnetic iron oxides for the site specific radio-frequency-induced hyperthermia of cancer. Journal of Magnetism and Magnetic Materials, 122: 374-378.

Charles S.W. and Popplewell J. (1980). Progress in the development of ferromagnetic liquids. Institute of Electrical and Electronics Engineers for Transmission Magnetism, 16: 172-177.

Chatterjee J., Haik Y. and Chen C.J. (2003). Size dependent magnetic properties of iron oxide nanoparticles. Journal of Magnetism and Magnetic Materials, 257: 113-118.

Chen D.H. and Liao M.H.(2002). Preparation and characterization of YADH-bound magnetic nanoparticles. Journal of Molecular Catalysis B: Enzymatic, 16: 283-291.

Chen D.H. and Wu S.H. (2000). Synthesis of nickel nanoparticles in water-in-oil microemulsions. Chemistry of Materials, 12: 1354-1360.

Chen M., Yamamuro S., Farrell D. and Majetich S.A. (2003). Gold-coated iron oxide for biomedical applications. Journal of Applied Physics, 93: 7551-7553.

Chin A.B. and Yaacob I.I. (2007). Synthesis and characterization of magnetic iron oxide nanoparticles via w/o micro emulsion and massart's procedure. Journal of Materials Processing Technology, 191: 235-237.

Cunningham C.H., Arai T., Yang P.C., McConell M.V., Pauly J.M. and Conolly S.M. (2005). Positive contrast magnetic resonance imaging of cells labelled with magnetic nanoparticles. Magnetic Resonance in Medicine, 53: 999-1005.

Davis R. (2001). Particle science and technology-a view at the millennium. Powder Technology, 119: 45.

Del Barco E., Asenjo J., Zhang X.X., Pieczynsky R., Julia A., Tejada J., Ziolo R.F., Fiorani D. and Testa A.M. (2001). Free rotation of magnetic nanoparticles in a solid matrix. Chemistry of Materials, 13: 1487-1490.

Duncan R. and Izzo L. (2005). Dendrimer biocompatibility and toxicity. Advanced Drug Delivery Reviews, 57: 2215-2237.

Ferrari M. (2005). Cancer nanotechnology: opportunities and challenges. Nature Reviews Cancer, 5: 161-171.

Fréchet J.M.J. (2005). Functional polymers: from plastic electronics to polymer-assisted therapeutics. Progress in Polymer Science, 30: 844-857.

Fu L., Dravid V.P. and Johnson D.L. (2001). Self-assembly(SA) bilayer molecular coating on magnetic nanoparticles. Applied Surface Science, 181: 173-178.

Gao Y., Chen B., Li H. and Ma Y. (2003). Preparation and characterization of a magnetically separated photocatalyst and its catalytic properties. Materials Chemistry and Physics, 80: 348-355.

Gomez-Lopera S.A., Plaza R.C. and Delgado A.V. (2001). Synthesis and characterization of spherical magnetite/biodegradable polymer composite particles. Journal of Colloid and Interface Science, 240: 40-47.

Gong J.L., Huang Y., Chen J.W., Jiang J.H., Shen J.L. and Yu R.Q. (2007). Ag/SiO2 core-shell nanoparticle based surface-enhacnced Raman probes for immunoassay of cancer marker using silica-coated magnetic nanoparticles as separation tools. Biosensors and Bioelectronics, 22: 1501-1507.

Gordon R.T., Hines J.R. and Gordon D. Intracellular hyperthermia. A biophysical approach to cancer treatment via intracellular temperature and biophysical alterations. Medical Hypothesis, 5: 83-102.

Goya G.f., Berquo T.S. and Fonseca F.C. (2003). Static and dynamic magnetic properties of spherical magnetite nanoparticles. Journal of Applied Physics, 94: 3520-3528.

Gupta A.K. and Curtis A.S.G. (2003). Lactoferrin and ceruloplasmin derivatized superparamagnetic iron oxide nanoparticles: preparation, characterization and their

influence on human dermal fibroblasts in culture. Proceedings of the 30th Annual Symposium of Controlled Release of Bioactive Materials, 30: 788

Gupta A.K., Berry C., Gupta M. and Curtis A. (2003). Receptor-mediated targeting of magnetic nanoparticles using insulin as a surface ligand to prevent endocytosis. Institute of Electrical and Electronics Engineers for Transmission Nanobiosciences, 2: 256-261.

Gupta A.K. and Curtis A.S.G. (2004). Lactoferrin and ceruloplasmin derivatized superparamagnetic iron oxide nanoparticles for targeting cell surface receptors. Biomaterials, 25: 3029-40.

Gupta A.K. and Gupta M. (2005). Synthesis and surface engineering of iron oxide nanoparticles for biomedical applications. Biomaterials, 26: 3995-4021.

Gupta A.K. and Wells S. (2004). Surface-modified superparamagnetic nanoparticles for drug delivery: Preparation, characterization, and cytotoxicity studies. Institute of Electrical and Electronics Engineers for Transmission Magnetism. Nanobiosciences, 3: 66-73.

Gupta P.K. and Hung C.T. (1989). Magnetically controlled targeted micro carrier systems. Life Sciences, 44: 175-86.

Guzmán M.G., Dille J. and Godet S. (2008). Synthesis of silver nanoparticles by chemical reduction method and their antibacterial activity. Proceedings of World Academy of Science, Engineering and Technology, 33: 2070-3740.

Häfeli U.O. (2004). Magnetically modulated therapeutic systems. International Journal of Pharmaceutics, 277: 19-24.

Hamley I.W. (2003). Nanotechnology with soft materials. Angew Chemical International Education, 42: 1692-712.

Han D.H., Wang J.P. and Luo H.L. (1994). Crystallite size effect on saturation magnetization of fine ferromagnetic particles. Journal of Magnetism and Magnetic Materials, 136: 176-182.

Handgretinger R., Lang P., Schumm M., Taylor G., Neu S., Koscielnak E., Niethammer D. and klingebiel T. (1998). Isolation and transplantation of autologous peripheral CD34+ progenitor cells highly purified by magnetic-activated cell sorting. Bone Marrow Transplant, 21: 987-993.

Hooper C. (2000). Dye and let live: magtags emerging as cellular compass. National Intitutes of Health Catalyst, 8: 15256-15261.

Iacob G.H., Rotariu O., Strachan N.J.C. and Häfeli U.O. (2004). Magnetizable needles and wires-modelling and efficient way to target magnetic microspheres in vivo. Biorheology, 41: 599-612.

Jemal A., Siegel R., Ward E., Murray T., Xu J. and Thun M.J. (2007). Cancer Statistics. A Cancer Journal for Clinicians, 57: 43-66.

Jin Y., Dennis C.L. and Majetich S.A. (1999). Nanoscale characterization of magnetic nanoparticles. Nanostructured Materials, 12: 763-768.

Johannsen M., Gneveckow U., Eckelt L., Feussner A., Scholz R., Deger S., Wust P., Loening S.A. and Jordan A. (2005). Clinical hyperthermia of prostate cancer using magnetic nanoparticles: presentation of a new interstitial technique. International Journal of Hyperthermia, 21: 637-647.

Johnson G.A. (1993). Histology by magnetic resonance microscopy. Magnetic Resonance, Q9: 1-30.

Jurgons R., Seliger C., Hilpert A., Trahms I., Odenbach S. and Alexiou C. (2006). Drug loaded magnetic nanoparticles for cancer therapy. Journal of Physics: Condensed Matter, 18: S2893-S2902.

Khalafalla S.E. and Reimers G.W. (1980). Preparation of dilution-stable aqueous magnetic fluids. Institute of Electrical and Electronics Engineers for Transmission Magnetism, 16: 178-183.

Kim D.K., Zhang Y., Voit W., Rao K.V. and Muhammed M. (2001). Synthesis and characterization of surfactant-coated superparamagnetic monodispersed iron oxide nanoparticles. Journal of Magnetism and Magnetic Materials, 225: 30-36.

Kim K.C., Kim E.K., Lee J.W., Maeng S.L. and Kim Y.S. (2008). Synthesis and characterization of magnetite nanopowders. Current Applied Physics, 8: 758-760.

Kinoshita T., Seino S., Okitsu K., Nakayama T., Nakagawa T. and Yamamoto T.A. (2003). Journal of Alloys and Compounds, 359: 46-50.

Kinoshita T., Seino S., Mizukoshi Y., Nakagawa T. and Yamamoto T.A. (2007). Functionalization of magnetic gold/iron-oxide composite nanoparticles with oligonucleotides and magnetic separation of specific target. Journal of Magnetism and Magnetic Materials, 311: 255-258.

Krotz F., Wit C., Sohn H.Y., Zahler S., Gloe T., Pohl U. and Plank C. (2003). Magnetofection-a highly efficient tool for antisense oligonucleotide delivery in vitro and in vivo. Molecular Therapy, 7: 700-710.

Kubo T., Sugita T., Shimose S., Nitta Y., Ikuta Y. and Murakami T. (2001). Targeted systematic chemotherapy using magnetic liposomes with incorporated adriamycin for osteosarcoma in hamsters. International Journal of Oncology, 18: 121-125.

Kubo T., Sugita T., Shimose S., Nitta Y., Ikuta Y. and Murakami T. (2000). Targeted delivery of anticancer drugs with intravenously administered magnetic liposomes in asteosarcoma-bearing hamsters. International Journal of Oncology, 17: 309-315.

LaConte L., Nitin N. and Bao G. (2005). Magnetic nanoparticle probes. Nanotoday, 32: 32-38.

Lee Y., Lee J., Bae C.J., Park J.G., Noh. and Park J.H. (2005). Large-scale synthesis of uniform and crystalline magnetite nanoparticles using reverse micelles as nanoreactors under reflux conditions. Advanced Functional Materials, 15: 503-509.

Lee J., Isobe T. and Senna M. (1996). Preparation of ultrafine Fe_3O_4 particles by precipitation in the presence of PVA at high pH. Journal of Colloid and Interface Science, 177: 490-494.

Lefebure S., Dubois V., Cabuil V., Neveu. and Massart S. (1998). Monodisperse magnetic nanopaticles: preparation and dispersion in water and oils. Journal of Materials Research, 10: 2975.

Li Y., Xiong P., Molnár S.V., Wirth S., Ohno Y. and Ohno H. (2002). Hall magnetometry on a single iron nanoparticle. Applied Physics Letters, 80: 4644-4646.

Lim J., Tilton R.D., Eggeman A. and Majetich S.A. (2007). Design and synthesis of plasmonic magnetic nanoparticles. Journal of Magnetism and Magnetic Materials, 311: 78-83.

Lin J., Zhou W., Kumbhar A., Fang J., Carpenter E.E. and O'Connor C.J. (2001). Gold-coated iron (Fe@Au) nanoparticles: synthesis, characterization, and magnetic field-induced self-assembly. Journal of Solid State Chemistry, 159: 26-31

Liu Z., Liu Y., Yang Y., Shen G. and Yu R. (2005). A phenol biosensor based on immobilizing tyrosinase to modified core-shell magnetic nanoparticles supported at a carbon paste electrode. Analytica Chimica Acta, 533: 3-9.

Liu Z.L., Ding Z.H., Yao K.L., Tao J., Du G.H., Lu Q.H., Wang X., Gong F.L. and Chen X. (2003). Preparation and characterization of polymer-coated core-shell structured magnetic microbeads. Journal of Magnetism and Magnetic Materials, 265: 98-105.

Liu Z.M., Yang H.F., Li Y.F., Liu Y.L., Shen G.L. and Yu R.Q. (2006). Core-shell magnetic nanoparticles applied for immobilization of antibody on carbon paste electrode and amperometric immunosensing, Sensors and Actuators B. Chemical, 113: 956-962.

Liu X., Guan Y., Ma Z. and Liu H. (2004). Surface modification and characterization of magnetic polymer nanospheres prepared by miniemulsion polymerization. Langmuir, 20: 10278-10282.

Lobel B., Eyal O., Kariv N. and Katzir A. (2000). Temperature controlled CO_2 laser welding of soft tissues: Urinary bladder welding in different animal model (rats, rabbits, and cats). Lasers in Surgery and Medicine, 26: 4-12.

Lopez-Quintela M.A. and Rivas J. (1993). Chemical reactions in microemulsions: A powerful method to obtain ultrafine particles. Journal of Colloid Interface Sciences, 158: 446-451.

Lu Q.H., Yao K.L., Xi D., Liu Z.L., Luo X.P. and Ning Q. (2006). Synthesis and characterization of composite nanoparticles comprised of gold shell and magnetic core/cores. Journal of Magnetism and Magnetic Materials, 301(1): 44-49.

Lübbe A.S., Alexiou C. and Bergemann C. (2001). Clinical applications of magnetic drug targeting. Journal of Surgical Research, 95: 200-206.

Lübbe A.S., Bergemann C., Brock J. and McClure D.G. (1999). Physiological aspects in magnetic drug-targeting. Journal of Magnetism and Magnetic Materials, 194: 149-155.

Luderer A.A., Borreli N.F., Panzarino J.N., Mansfield G.R., Hess D.M., Brown J.L. and Barnett E.H. (1983). Glass-ceramic-mediated, magnetic-field-induced localized hyperthermia: response of a murine mammary carcinoma. Radiation Resolution, 94: 190-198.

Lyon J.L., Fleming D.A., Stone M.B., Schiffer P. and William M.E. (2004). Synthesis of Fe oxide core/Au shell nanoparticles by iterative hydroxyl amine seeding. Nano Letters, 4: 719-723.

Macaroff P.P., Simioni A.R., Lacava Z.G.M., Lima E.C.D., Morais P.C. and Tedesco A.C. (2006). Studies of cell toxicity and binding of magnetic nanoparticles with blood stream macromolecules. Journal of Applied Physics, 99: 08S102.

Maity D. and Agrawal D.C (2007). Synthesis of iron oxide nanoparticles under oxidizing environment and their stabilization in aqueous and non-aqueous media. Journal of Magnetism and Magnetic Materials, 308: 46-55.

Maity D., Choo S.G., Yi J., Ding J. and Xue J.M. (2009). Synthesis of magnetite nanoparticles via solvent-free thermal decomposition route. Journal of Magnetism and Magnetic Materials, 321: 1256-1259.

Mendenhall G.D., Geng Y. and Hwang J. (1996). Optimization of long-term stability of magnetic fluids from magnetite and synthetic polyelectrolytes. Journal of Colloid and Interface Science, 184: 519-526.

Moghimi S.M., Hunter A.C.H. and Murray J.C. (2001). Long-circulating and target specific nanoparticles: theory to practice. Pharmacological Reviews, 53: 283-318.

Mulvaney P., Liz-Marzán L.M., Giersig M. and Ung T. (2000). Silica encapsulation of quantum dots and metal clusters. Journal of Materials Chemistry, 10: 1259-1270.

Murakami Y., Shindo D., Oikawa K., Kainuma R. and Ishida K. (2002). Magnetic domain structures in Co-Ni-Al shape memory alloys studied by Lorentz microscopy and electron holography. Acta Materialia, 50: 2173-2184.

Neuberger T., Schöpf B., Hoffman H., Hoffmann M. and Rechenberg B.V. (2005). Superparamagnetic nanoparticles for biomedical applications: Possibilities and limitations of a new drug delivery system. Journal of Magnetism and Magnetic Materials, 293: 483-496.

Ng V., Lee Y.V., Chen B.T. and Adeyeye A.O. (2002). Nanostructure array fabrication with temperature-controlled self-assembly techniques. Nanotechnology, 13: 554-558.

Nielsen O.S., Horsman M. and Overgaard J. (2001). A future for hyperthermia in cancer treatment. European Journal of Cancer, 37: 1587-1589.

Nishimaki K., Yamamoto T.A., Nakagawa T. and Katsura M. (2000). Japanese Journal of Applied Physics, 39: 1225.

Nitin N., LaConte L.E.W., Zurkiya O., Hu X. and Bao G. (2004). Functionalization and peptide-based delivery of magnetic nanoparticles as an intracellular MRI contrast agent. Journal of Biological Inorganic Chemistry, 9: 706-712.

Olsvik O., Popovic T., Skjerve E., Cudjoe K.S., Hornes E., Ugelstad J. and Ulhen M. (1994). Magnetic separation techniques in diagnostic microbiology. Clinical Microbiology Reviews, 7: 43-54.

Pankhurst Q.A., Conolly J., Jones S.K. and Dobson J. (2003). Applications of magnetic nanoparticles in biomedicine. Journal of Physics D: Applied Physics, 36: R167-R181.

Park J.I. and Cheon J. (2001). Synthesis of "solid solution" and "core-shell" type cobalt-platinum magnetic nanoparticles via transmetalation reactions. Journal of the American Chemical Society, 123: 5743-5746.

Park S.I., Lim J.H., Kim J.H., Yun H.I. and Kim C.O. (2006). Toxicity estimation of magnetic fluids in a biological test. Journal of Magnetism and Magnetic Materials, 304: e406-e408.

Petit C., Taleb A. and Pileni M.P. (1998). Self-organization of magnetic nanosized cobalt particles. Advanced Materials, 10: 259-261.

Pham T.T.H., Cao C. and Sim S.J. (2008). Application of citrate-stabilized gold-coated ferric oxide composite nanoparticles for biological separations. Journal of Magnetism and Magnetic Materials, 320: 2049-2055.

Presa P., Multigner M., Morales M.P., Rueda T., Fernández-Pinel P. and Hernando A. (2007). Synthesis and characterization of FePt/Au core-shell nanoparticles. Journal of Magnetism and Magnetic Materials, 316: e753-e755.

Qiu X. (2000). Synthesis and characterization of magnetic nanoparticles. Chinese Journal of Chemistry, 18: 834-837.

Reamer P. and Weissleder R. (1996). Development and experimental application of receptor-specific MR contrast media. Radiology, 36: 153-63.

Reimers G.W. and Khalafalla S.E. (1972). Preparing magnetic fluids by a peptizing method. US Bureau Mines Technical Representative: 59.

Roberts M.J., Bentley M.D. and Harris J.M. (2002). Chemistry of peptide and protein PEGylation. Advanced Drug Delivery Reviews, 54: 459-476.

Rockenberger J., Scher E.C. and Alivisators A.P. (1999). A new nonhydrolytic single-precursor approach to surfactant-capped nanocrystals of transition metal oxides. Journal of American Chemical Society, 121: 11595-11596.

Rotariu O. and Strachani N.J.C. (2005). Modeling magnetic carrier particle targeting in the tumor microvasculature for cancer treatment. Journal of Magnetism and Magnetic Materials, 293: 639-646.

Sahoo Y., Pizem H., Fried T., Golodnitsky D., Burstein L., Sukenik C.N. and Markovich G. (2001). Alkyl phosphonate/phosphate coating on magnetite nanoparticles: a comparison with fatty acids. Langmuir, 17: 7907-7911.

Santra S., Tapec R., Theodoropoulou N., Dobson J., Hebard A. and Tan W. (2001). Synthesis and characterization of silica-coated iron oxide nanoparticles in microemulsion: the effect of non-ionic surfactants. Langmuir, 17: 2900-2906.

Satoshi S., Kinoshita T., Otome Y., Nakagawa T., Okitsu K., Mizukoshi Y., Nakayama T., Sekino T., Niihara K. and Yamamoto T.A. (2005). Gamma-ray synthesis of magnetic nanocarrier composed of gold and magnetic iron oxide. Journal of Magnetism and Magnetic Materials, 293: 144-150.

Sato T., Iijima T., Sekin M. and Inagaki N. (1987). Magnetic properties of ultrafine ferrite particles. Journal of Magnetism and Magnetic Materials, 65: 252.

Scherer F., Anton M., Schilinger U., Henke J., Bergemann C., Kruger A., Gansbacher B. and Plank C. (2002). Magnetofection: enhancing and targeting gene delivery by magnetic force in vitro and in vivo. Gene Therapy, 9: 102-109.

Schoepf U., Marecos E., Jain R. and Weissleder R. (1998). Intracellular magnetic labeling of lymphocytes for in vivo trafficking studies. Bio Techniques, 24: 642-651.

Schwertmann T. and Cornell R.M. (1991). Iron oxides in the laboratory: Preparation and characterization, VCH, Weinheim, Cambridge, 137: 11.

Sehlotho N., Nyokong T., Zagal J.H. and Bedioui F. (2006). Electrocatalysis of oxidation of 2-mercaptoethanol, i-cysteine and reduced glutathione by adsorbed and electrodeposited cobalt tetra phenoxypyrrole and tetra ethoxythiophene substituted phthalocyanines. Electrochimica Acta, 51: 5125-5130.

Seino S., Kinoshita T., Otome Y., Nakagawa T., Okitsu K., Mizukoshi Y., Nakayama T., Sekino T., Niihara K. and Yamamoto T.A. (2005). Gamma-ray synthesis of magnetic nanocarrier composed of gold and magnetic iron oxide. Journal of Magnetism and Magnetic Materials, 293: 144-150.

Seisdedos F.A. and Parmentier M. (2006). Genetics of resistance to HIV infection: Role of core-receptors and core-receptors ligands. Seminars in Immunology, 18: 387-403.

Seto T., Koga k., Takano F., Akinaga H., Ori T., Hirasawa M. and Murayama M. (2006). Synthesis of magnetic $CoPt/SiO_2$ nano-composite by pulsed laser ablation. Journal Photochemistry and Photobiology A: Chemistry, 182: 342-345.

Shafi K.V.P.M., Gedanken A., Prozorov R. and Balogh J. (1998). Sonochemical preparation and size dependent properties of nanostructured $CoFe_2O_4$ particles. Chemistry of Materials, 10: 3445-3450.

Sjogren C.E., Briley-Saebo K., Hanson M. and Johansson C. (1994). Magnetic characterization of iron oxides for magnetic resonance imaging. Magnetic Resonance in Medicine, 31: 268-272.

Sokolov K., Follen M., Aaron J., Pavlova I., Malpica A., Lotan R. and Richards-Kortum R. (1999-2004). Real-time vital optical imaging of pre-cancer using anti-epidermal growth factor receptor antibodies conjugated to gold nanoparticles. Cancer Research, 63: 1999-2004.

Sugimoto T. and Matijevi E. (1980). Formation of uniform spherical magnetite particles by crystallization from ferrous hydroxide gels. Journal of Colloid Interface Sciences, 74: 227-243.

Sun S. and Zeng H. (2002). Size-controlled synthesis of magnetite nanoparticles. Journal of American Chemical Society, 124: 8204-8205.

Sunderland C.J., Steiert M., Talmadge J.E., Derfus A.M. and Barry S.E. (2006). Targeted nanoparticles for detecting and treating cancer. Drug Development Research, 67: 70-93.

Tadmor R., Rosensweig R.E., Frey J. and Klein J. (2000). Resolving the puzzle of ferrofluid dispersants. Langmuir, 16: 9117-9120.

Taleb A., Petit C. and Pileni M.P. (1997). Synthesis of highly monodisperse silver nanoparticles from AOT reverse micelles: A way to 2D and 3D self-organization. Chemistry of Materials, 9: 950-959.

Tanaka M., Misaka Y., Shiomi K., Yamamoto T.A., Nakagawa T., Katsura M., Numazawa T., Nakayama T. and Niihara K. (2001). Scripture Material, 44: 2141.

Tang J., Myers M., Bosnick K.A. and Brus L.E. (2003). Magnetic Fe_3O_4 nanocrystals: spectroscopic observation of aqueous oxidation kinetics. The Journal of Physical Chemistry B, 107: 7501-7506.

Tarjaj P. and Serna C. (2003). Synthesis of monodisperse superparamagnetic Fe/silica nanospherical composites. Journal of American Chemical Society, 125: 15754-15755.

Tarjaj P., Morales M.P., Verdaguer S., Carreno T. and Serna C.J. (2003). The preparation of magnetic nanoparticles for applications in biomedicine. Journal of Physics D: Applied Physics, 36: R182-R197.

Tartaj P., González-Carreño T. and Serna C.J. (2002). Synthesis of nanomagnets dispersed in colloidal silica cages with applications in chemical separation. Langmuir, 18: 4556-4558.

Tartaj P., Gonzálenz-Carreño T. and Serna C.J. (2001). Single-step nanoengineering of silica coated maghemite hollow spheres with tunable magnetic properties. Advanced Materials, 13: 1620-1624.

Tepper T., Ilievski F., Ross C.A., Zaman T.R., Ram R.J., Sung S.Y. and Stadler B.J.H. (2003). Magneto-optical properties of iron oxide films. Journal of Applied Physics, 93: 6948-6950.

Tie S.L., Lee H.C., Bae Y.S., Kim M.B., Lee K.and Lee C.H. (2007). Monodisperse Fe3O4 core/shell nanoparticles with enhanced magnetic property, colloids and surfaces A: Physicochemical and Engineering Aspects, 293: 278-285.

Tillotson T.M., Gash A.E., Simpson R.L., Hrubesh L.W. and Satcher J.H. (2001). Nanostructured energetic materials using sol-gel methodologies. Journal of Non-Crystalline Solids, 285: 335-338.

Tomalia D.A. (2005). Birth of a new macromolecular architecture: dendrimers as quantized building blocks for nanoscale synthetic polymer chemistry. Progress in Polymer Science, 30: 294-324.

Torchilin V.P. and Trubetskoy V.S. (1995). Which polymers can make nanoparticulate drug carriers long-circulating. Advanced Drug Delivery Reviews, 16: 141-155.

Tourinho F., Franck R., Massart R. and Perzynski R. (1989). Synthesis and magnetic properties of manganese and cobalt ferrofluids. Progress in Colloid and Polymer Science, 79: 128.

Ugelstad J., Stenstad P., Kilaas L., Prestvik W.S., Herje R., Bererge A. and Hornes E. (1993). Monodisperse magnetic polymer particles. New biochemical and biomedical applications. Blood Purification, 11: 349-369.

Ulman A. (1996). Formation and structure of self-assembly monolayers. Chemical Reviews, 96: 1533-1554.

Vayssieres L., Chanei C., Tronc E. and Jolivet J.P. (1998). Size tailoring for magnetite particles formed by aqueous precipitation: an example of thermodynamic stability of nanometric oxide particles. Journal of Interface Science, 205: 205-212.

Vestal C.R. and Zhang Z.J. (2002). Atom transfer radical polymerization synthesis and magnetic characterization of $MnFe_2O_4$ polystyrene core shell nanoparticles. Journal of the American Chemical Society, 124: 14312-14313.

Vlamidir S., Zaitsev V., Dmitry S., Filimonov I., Gambino R.J., Chu B. and Presnyakov A. (1999). Physical and chemical properties of magnetite and magnetite-polymer nanoparticles and their colloidal dispersions. Journal of Colloid and Interface Science, 212: 49.

Voit W., Kim D.K., Zapka W., Muhammed M. and Rao K.V. (2001). Magnetic behavior of coated superparamagnetic iron oxide nanoparticles in ferrofluids. Materials Research Society, 676: Y7.8.1-6.

Wagner J., Autenrieth T. and Hempelmann R. (2002). Core shell particles consisting of cobalt ferrite and silica as model ferrofluids [$CoFe_3O_4$-SiO_2 core shell particles]. Journal of Magnetism and Magnetic Materials, 252: 4-6.

Wang J.H.H., Dravid V.P., Teng M.H., Host J.J., Elliot B.R., Johnson D.L. and Mason T.O. (1997). Magnetic properties of graphitically encapsulated nickel nanocrystals. Journal of Material Research, 12: 1076.

Wang Y. and Lee J.K. (2007). Recyclable nano-size Pd catalyst generated in the multilayer polyelectrolyte films on the magnetic nanoparticle core. Journal of Molecular Catalysis A: Chemical, 263: 163-168.

Waniewska A.S., Gutowski M. and Lachowicz H.K. (1992). Superparamagnetism in a nanocrystalline Fe-based metallic glass. Physical Review, B46: 14594-14597.

Weissleder R., Cheng H.C., Bogdanova A. and Bogdanov A. (1997). Magnetically labeled cells can be detected by MR imaging. Journal of Magnetic Resonance Imaging, 7: 258-263.

Weissleder R., Bogdanov A., Neuwelt E.A. and Papisov M. (1995). Long circulating iron oxides for MR imaging. Advanced Drug Delivery Reviews, 16: 321-334.

Widder K.J., Morris R.M., Poore G., Howard D.P.Jr. and Senyei A.E. (1981). Tumor remission in Yoshida sarcoma-bearing rats by selective targeting of magnetic albumin microspheres containing doxorubicin. Proceedings of the National Academic of Sciences, 78: 579-581.

Winnik F.M., Morneau A., Ziolo R.F., Stover H.D.H. and Li W.H. (1995). Template-controlled synthesis of superparamagnetic goethite within microporous polymetric microspheres. Langmuir, 11: 3660-3666.

Wu X., Jin G., Guan L., Cao H. and Guo X.Y. (2006). Preparation and characterization of core-shell structured α-Fe_2O_3/SiC spheres. Materials Science and Engineering: A, 433: 190-194.

Xu H.H., Smith D.T. and Simon C.G. (2004). Strong and bioactive composites containing nano-silica-fused whiskers for bone repair. Biomaterials, 25: 4615-4626.

Yaacob I.I., Nunens A.C., Bose A. and Shah D.O. (1994). Synthesis and characterization of magnetic nanoparticles in spontaneously generated vesicles. Journal of Colloid Interface Sciences, 168: 289-301.

Yamamoto T.A., Tanaka M., Misaka Y., Nakagawa T., Nakayama T., Niihara K. and Numazawa T. (2002). Dependence of the magnetocaloric effect in superparamagnetic nanocomposites on the distribution of magnetic moment size. Scripture Materials, 46: 89-94.

Yamamoto T.A., Nishimaki K., Harabe T., Shiomi K., Nakagawa T. and Katsura M. (1999). Magnetic composites composed of iron-nitride nanograins dispersed in silver matrix. Nano Structured Materials, 12: 523.

Yamamoto T., Croft M.C., Shull R.D. and Hahn H.W. (1995). Phase Identification of a Superparamagnetic Iron-Oxide/Silver Nanocomposite. Nano Structured Materials, 6: 965-968.

Yamamoto T., Shull R.D., Bandaru P.R., Cosandey F. and Hahn H.W. (1994). Superparamagnetic nanocomposite of silver/iron-oxide by inert gas condensation. Japanese Journal of Applied Physics, 33: 1301.

Yee C., Kataby G., Ulman A., Prozorov T., White H., King A., Rafailovich M., Sokolov J. and Gedanken A. (1999). Self assembly monolayers of alkanesulfonic and phosphonic acids on amorphous iron oxide nanoparticles. Langmuir, 15: 7111.

Yeh T.C., Zhang W., Ldstad S.T. and Ho C. (1993). Intracellular labeling of T-cells with suparparamagnetic contrast agents. Magnetic Resonance in Medicine, 30: 617-625.

Yellen B.B., Forbes Z.G., Halverson D.S., Fridman G., Barbee K.A., Chorny M. and Levy R. (2005). Targeted drug delivery to magnetic implants for the therapeutic applications. Journal of Magnetism and Magnetic Materials, 293: 647-654.

Yin H., Too H.P. and Chow G.M. (2005). The effects of particle size and surface coating on the cytotoxicity of nickel ferrite. Biomaterials, 26: 5818-5826.

Yonglan L. (2007). One-step preparation of gold nanoparticles with different size distribution. Materials Letters, 61: 1039-1041.

Zaitsev V., Filimonov D.S., Preshyakov I.A., Gambino R.J. and Chu B. (1999). Physical and chemical properties of magnetite and magnetite-polymer nanoparticles and their colloidal dispersions. Journal of Colloid and Interface Science, 212: 49-57.

Zhang S., Dong D., Sui Y., Liu Z., Wang H., Qian Z. and Su W. (2006). Preparation of core shell particles consisting of cobalt ferrite and silica by sol-gel process. Journal of Alloys and Compounds, 415: 257-260.

Zhang Y., Zeng G.M., Tang L., Huang D.L., Jiang X.Y. and Chen Y.N. (2007). A hydroquinone biosensor using modified core-shell magnetic nanoparticles supported on carbon paste electrode. Biosensors and Bioelectronics, 22: 2121-2126.

Zhang X.F., Dong X.L., Huang H., Lv B., Zhu X.G., Lei J.P., Ma S., Liu W. and Zhang Z.D. (2007). Synthesis, structure and magnetic properties of SiO_2-coated Fe nanocapsules. Materials Science and Engineering A, 454-455: 211-215.